

# Phase-coherence and the boson-analogy of vortex liquids

A. K. Nguyen and A. Sudbø

*Department of Physics*

*Norwegian University of Science and Technology, N-7034 Trondheim, Norway*

The statistical mechanics of the flux-line lattice in extreme type-II superconductors is studied within the framework of the uniformly frustrated anisotropic three-dimensional  $XY$ -model. It is assumed that the externally applied magnetic field is low enough to invalidate the lowest Landau-level approach to the problem. A finite-field counterpart of an Onsager vortex-loop transition in extreme type-II superconductors renders the vortex liquid phase-incoherent when the Abrikosov vortex lattice undergoes a first order melting transition. For the magnetic fields considered in this paper, corresponding to filling fractions  $f$  given by  $1/f = 12, 14, 16, 20, 25, 32, 48, 64, 72, 84, 96, 112,$  and  $128$ , the vortex liquid phase is not describable as a liquid of well-defined field-induced vortex lines. This is due to the proliferation of thermally induced closed vortex-loops with diameters of order the magnetic length in the problem, resulting in a “percolation transition” driven by non-field induced vortices also *transverse* to the direction of the applied magnetic field. This immediately triggers flux-line lattice melting and loss of phase-coherence along the direction of the magnetic field. Due to this mechanism, the field induced flux lines loose their line tension in the liquid phase, and cannot be considered to be directed or well defined. In a non-relativistic  $2D$  boson-analogy picture, this latter feature would correspond to a vanishing mass of the bosons. Scaling functions for the specific heat are calculated in zero and finite magnetic field. From this we conclude that the critical region is of order 10% of  $T_c$  for a mass-anisotropy  $\sqrt{M_z/M} = 3$ , and increases with increasing mass-anisotropy. The entropy jump at the melting transition is calculated in two ways as a function of magnetic field for a mass-anisotropy slightly lower than that in  $YBCO$ , namely with and without a  $T$ -dependent prefactor in the Hamiltonian originating at the microscopic level and surfacing in coarse grained theories such as the one considered in this paper. In the first case, it is found to be  $\Delta S = 0.1k_B$  per pancake-vortex, roughly independent of the magnetic field for the filling fractions considered here. In the second case, we find an enhancement of  $\Delta S$  by a factor which is less than 2, increasing slightly with decreasing magnetic field. This is still lower than experimental values of  $\Delta S \approx 0.4k_B$  found experimentally for  $YBCO$  using calorimetric methods. We attribute this to the slightly lower mass-anisotropy used in our simulations.

Pacs-numbers: 74.20.De, 74.25.Dw, 74.25.Ha, 74.60.Ec

## I. INTRODUCTION

The physics of vortex matter represents a new field of research, which has opened up after the discovery of large fluctuation effects in the extreme type-II high- $T_c$  superconductors. In particular, the work of Gammel *al.*<sup>1</sup> and Nelson<sup>2</sup> were important milestones in the field, suggesting for the first time that the Abrikosov vortex lattice might melt *well below* the zero-field critical temperature. This extension of ideas originally proposed by Eilenberger<sup>3</sup>, has proved to be fruitful. The melting of the flux-line lattice (FLL) well below the upper critical field crossover line due to large anisotropy combined with extreme nonlocality of vortex-vortex interactions<sup>4</sup>, as well as its first order character, are now well established both on theoretical and experimental grounds. Nonetheless, the nature of the molten phase remains tantalizingly elusive. Obviously, there exists a  $2D$  boson analogy picture of the low-temperature phase of the FLL, where the corresponding boson system is an insulating one. This is nothing but Abrikosov’s mean-field solution to the problem<sup>5</sup>. There is, however, mounting analyt-

ical and numerical evidence that a similar, intuitively appealing, picture of the molten phase via a  $2D$  *non-relativistic* superfluid boson system<sup>2</sup>, may need a substantial revision<sup>6–10</sup>. As far as experimental results are concerned, the situation also appears quite intriguing<sup>11</sup>.

At issue here is to what extent the well-defined flux lines of the low-temperature FLL phase retain their integrity in the high-temperature molten phase. In this paper, we address the issue of the character of the vortex liquid via extensive Monte-Carlo simulations of the uniformly frustrated three-dimensional  $XY$  ( $3DXY$ ) model.

An issue of fundamental importance is whether or not a vortex liquid (the molten phase of the FLL) is a superconductor or not when the vortex system is not pinned. It is clear that the superfluid response to a current applied transversely to the field induced vortices is zero at all temperatures, provided that pinning is absent. In the perfect FLL there will however be a superfluid response to a current applied parallel to the magnetic field. There remains the possibility that a finite superfluid response might remain even in the liquid phase for this geometry, and that it may vanish only deep in the vortex

liquid as suggested originally by Feigel'man *et al.*<sup>12</sup>. A main point of this paper is to show that for the moderate mass-anisotropy and large range of magnetic fields considered here, this in fact does not appear to be the case. Moreover, the reason that this is so has important consequences for the physical picture of the vortex liquid phase. Below, we give a summary of the main results of this paper.

The specific heat is calculated for filling fractions  $f = 1/12, \dots, 1/128, 0$ , and the results are found to be in good agreement with the experimental results of Salamon *et al.*<sup>13</sup> and more recent experiments of Roulin *et al.*<sup>14</sup>, and Schilling *et al.*<sup>15,16</sup>. In particular, we find that the near-logarithmic singularity in zero magnetic field (the specific heat exponent  $\alpha = -0.007$ ) is converted to a broad crossover with a peak value suppressed rapidly compared to the zero field case. This crossover defines, somewhat arbitrarily, the upper critical magnetic field. The entropy associated with the suppression of the specific heat at the crossover is partly compensated by the appearance of a  $\delta$ -function anomaly in the specific heat at temperatures well below the zero-field critical temperature. Such a  $\delta$ -function peak is identified unambiguously with the first order melting transition of the FLL. The field dependence of the temperature at which this appears defines the melting line of the FLL in the  $B - T$ -phase diagram of the superconductor. The field dependence of the entropy of the transition is found to be  $\Delta S \sim B$ , consistent with the suppression of the broad main crossover peak in the specific heat. This implies that the entropy per vortex per layer is essentially field independent in the field range and anisotropy range investigated here. We emphasize that the anisotropy considered,  $\sqrt{M_z/M} = 3$ , is moderate and somewhat smaller than what is found in YBCO. Nonetheless, the qualitative aspects of our results conform well with those found in YBCO<sup>15</sup>.

We find that in the field regime we have considered, i.e. fields down to  $B \sim 1 - 5T$ , the melting of the vortex lattice is triggered by a proliferation of thermally induced closed vortex rings of order the magnetic length of the system. This immediately leads to a ‘‘percolation’’ of vortex loops traversing the entire system in any given direction, and in particular in a direction perpendicular to the applied magnetic field. Hence, flux lines which are field induced, will traverse the entire system as it weaves its way from the bottom to the top of the system. In technical terms, in a simulation one needs to apply periodic boundary conditions at least once in the  $(x, y)$ -directions before a flux line starting at the center of the bottom layer has reached the top layer. *Therefore, it does not make sense to view the vortex liquid phase as a collection of well defined field-induced flux lines.* The above picture effectively means that the flux-line tension has vanished in the liquid phase. Within the 2D boson analogy picture, an equivalent statement would be that the boson mass, which is the analog of the line tension, has vanished<sup>17</sup>.

Scaling functions for the specific heat are calculated, in

zero field as well as in finite field. From the regime where scaling is found in zero field, we find the width of the critical region to be  $|T - T_c|/T_c \approx 0.1$  for a mass-anisotropy ratio  $\Gamma = \sqrt{M_z/M} = 3$ . This is considerably wider than what one would naively obtain using the Ginzburg-criterion. Moreover, this is slightly wider than what we have found for the isotropic case. The width of the critical region therefore increases slightly with mass anisotropy, for the moderate values of  $\Gamma$  we have considered. Vortex loops are expected to be particularly important for the statistical mechanics of the FLL, provided that the melting line is found in the proximity of the critical region. From the obtained melting curve and the width of the critical region, we find that the melting curve crosses the critical region curve at a field of order  $B = 1T$  for  $\Gamma = 3$ . Below this field, vortex loops will completely dominate the physics at the melting transition.

This paper is organized as follows. In section II we present the model, the approximations involved and the physical quantities considered, as well as updating procedure and the parameters used in our Monte Carlo simulations. In section III we present and discuss detailed results for the filling fraction  $f = 1/20$ . In section IV we present results in a broad range of filling fractions  $1/f \in [12, \dots, 128]$ . Section V presents the conclusions of this paper.

## II. THE MODEL

The phenomenological model considered in this paper for the high- $T_c$  cuprates, is the uniformly frustrated 3 dimensional anisotropic XY (3DXY) model on a lattice,<sup>18-20,8,9</sup> defined by the Hamiltonian

$$H(\{\theta(\mathbf{r})\}) = - \sum_{\mathbf{r}, \mu=x,y,z} J_\mu \cos[\nabla_\mu \theta(\mathbf{r}) - A_\mu(\mathbf{r})], \quad (1)$$

where  $\theta$  is the local phase of the superconducting complex order parameter and  $\nabla$  is a lattice derivative. Furthermore, the coupling energy along the  $\mu$ -axis,  $J_\mu$ , is defined by

$$J_x = J_y = \frac{\Phi_0^2 d}{16\pi^3 \lambda_{ab}^2} \equiv J_\perp, \quad J_z = \frac{\Phi_0^2 c^2}{16\pi^3 \lambda_c^2 d}.$$

Here  $\Phi_0$  is the flux quantum,  $\xi_{ab}$  is the superconducting coherence length within the CuO-planes, and  $d$  is the distance between two CuO-layers in adjacent unit cells. Furthermore,  $\lambda_{ab}$  and  $\lambda_c$  are the magnetic penetration lengths in the CuO planes, and along the crystals  $c$ -axis, respectively. In Eq. 1,  $A_\mu$  is related to the quenched vector potential  $\mathbf{A}_{vp}$  by

$$A_\mu(\mathbf{r}) \equiv \frac{2\pi}{\Phi_0} \int_{\mathbf{r}}^{\mathbf{r}+\hat{e}_\mu} d\mathbf{r}' \cdot \vec{A}_{vp}(\mathbf{r}'),$$

where  $\hat{e}_\mu$  is the unit vector along the  $\mu$ -axis. This  $3DXY$  model is dual to the anisotropic London model in the limit of  $(\lambda_{ab}, \lambda_c) \rightarrow \infty^{21}$ . This limit should be taken with the understanding that the coupling energies  $J_\perp$  and  $J_z$  are maintained finite. When  $(\lambda_{ab}, \lambda_c) \rightarrow \infty$ , gauge fluctuations are completely suppressed, leaving a quenched vector potential and uniform magnetic induction. Thus, the  $3DXY$  model should give an adequate description of the physics of extreme type-II single crystal superconductors in the field regime  $B_{c1} \ll B \ll B_{c2}$ . The condition  $B_{c1} \ll B$  ensures that the contribution to the magnetic induction from individual flux lines overlap strongly giving a uniform magnetic induction. The condition  $B \ll B_{c2}$  ensures that details of the internal structure of the vortex cores are not essential. Moreover, the  $3DXY$  model should give an adequate description of the physics of extreme type-II single crystal superconductors in zero-magnetic field when gauge fluctuations are not important.

In this paper we consider simple tetragonal systems with dimensions  $L_x = L_y = L_\perp$  and  $L_z$ . The coordinate  $(x, y, z)$ -axes are taken to be parallel to the crystal (a,b,c)-axes, respectively. We measure the in-plane length scales  $(x, y, L_x, L_y)$  in units of  $\xi_{ab}$  and the length scales along the  $z$ -axis  $(z, L_z)$  in units of  $d$ . Our unit cell is a simple tetragonal system with dimensions  $e_x = e_y = \xi_{ab}$ ,  $e_z = d$ . Periodic boundary conditions are used in all directions throughout.

### A. The internal energy and specific heat

The specific heat per site  $C$  is obtained using the standard fluctuation formula

$$\frac{C}{k_B} = \frac{1}{L_\perp L_z} \frac{\langle H^2 \rangle - \langle H \rangle^2}{(k_B T)^2}, \quad (2)$$

where  $k_B$  is Boltzmann's constant. Results for most temperatures are checked for consistency by differentiating the results for the internal energy with respect to temperature. To estimate the latent heat (entropy jump) at a first order phase transition, we consider the internal energy per site  $E$ ,

$$E = \frac{1}{L_\perp L_z} \langle H \rangle. \quad (3)$$

This expression holds as long as we do not include any  $T$ -dependence in the Hamiltonian. Such a  $T$ -dependence could conceivably arise in effective coarse-grained theories such as the GL-theory, as first pointed out in Ref.<sup>22</sup>. At a first order phase transition there is a discontinuity in the internal energy per site  $\Delta E$  associated with coexistence of the Abrikosov FLL phase and the vortex liquid. This in turn gives rise to a  $\delta$ -function peak in the specific heat<sup>8,9</sup>. For the melting transition of a vortex line lattice,  $\Delta E$  is related to the entropy jump per vortex lines per layer  $\Delta S$  by

$$\frac{\Delta S}{k_B} = \frac{\Delta E}{f k_B T_m}, \quad (4)$$

where  $T_m$  is the melting temperature and  $f$  is the vortex lines density defined below in Eq. 8. For consistency, one may also check this result by extracting the entropy jump at the melting transition from the scaling of the height of the  $\delta$ -function anomaly in the specific heat<sup>23,8,9</sup>

$$C = const + \frac{L^3}{4} \left( \frac{\Delta S}{k_B L^3} \right)^2. \quad (5)$$

### B. Scaling functions for the specific heat

An issue of principle importance is whether or not closed thermally induced vortex loops, i.e. the critical fluctuations, will influence the melting of the FLL. Naively, one expects this to be the case provided that the melting temperature  $T_m(B)$  is within the critical region of the zero-field transition. It is therefore a matter of interest to establish the width of the critical region of the anisotropic  $3DXY$ -model. To this end, we consider finite-size scaling of the specific heat. The region of data-collapse of the specific heat evaluated at various system sizes identifies the width of the critical region. It is also of interest to find the extension of this critical region to finite fields, i.e. the width of the crossover region around the upper critical field, and how it depends on the anisotropy ratio  $\Gamma$ . If the melting line is located within this crossover-region or close to it, one expects a vortex-loop "blowout"<sup>9,7</sup> to dominate the physics at the melting transition, analogous to what was suggested to happen in superfluid  $He^4$  by Onsager<sup>24</sup>. This is particularly important at very low magnetic fields, like those considered in the experiments of Zeldov *et al.*<sup>11</sup>.

For the zero-field finite-size scaling of the specific heat, we have used cubic samples  $L \times L \times L$  with  $L = 16, 32, 48, 64, 72, 96$  to avoid spurious geometric effects. To investigate the possibility that the width of the critical region may depend on anisotropy, we have considered the two cases  $\Gamma = 1$  and  $\Gamma = 3$ .

The finite-size scaling function for the specific heat may in general be obtained in standard fashion from the singular part of the free energy as<sup>25,26</sup>

$$C(t, L) = L^{\alpha/\nu} \Phi_\pm(|t|L^{1/\nu}),$$

or equivalently

$$\frac{C(t, L)}{C(t, \infty)} = G_\pm(|t|L^{1/\nu}),$$

where  $|t| = |T - T_c|/T_c$ , and where  $\Phi_\pm(|t|L^{1/\nu})$  and  $G_\pm(|t|L^{1/\nu})$  are analytic functions of their arguments. Here,  $\alpha$  is the specific heat critical exponent, and  $\nu$

is the critical exponent of the superconducting correlation length, hyperscaling yields  $\alpha = 2 - D\nu$  in a  $D$ -dimensional system. As discussed in detail in Ref.<sup>26</sup>, a more convenient scaling form for numerical purposes is given by

$$\frac{C(t, L) - C(0, \infty)}{C(0, L) - C(0, \infty)} = G_{\pm}(|t|L^{1/\nu}). \quad (6)$$

We will use this scaling form to determine the width of the critical region.

In the presence of a general field  $X$  with scaling dimension  $X \sim \xi^{-\lambda}$ , where  $\xi$  is the correlation length  $\xi \sim |t|^{-\nu}$ , we have

$$C(t, X) = |t|^{-\alpha} \mathcal{G}_{\pm}(X|t|^{-\lambda\nu}).$$

Subtracting out the zero-field part, and introducing  $y \equiv X|t|^{-\lambda\nu}$  and  $\Delta C(t, X) \equiv C(t, X) - C(t, 0)$ , we find

$$|t|^{\alpha} \Delta C(t, X) = \left[ \mathcal{G}_{\pm}(y) - \mathcal{G}_{\pm}(0) \right],$$

$$X^{\alpha/\lambda\nu} \Delta C(t, X) = y^{\alpha/\lambda\nu} \left[ \mathcal{G}_{\pm}(y) - \mathcal{G}_{\pm}(0) \right] \equiv \mathcal{H}_{\pm}(y).$$

Choosing  $X = B$ , the induction, implies that the scaling dimension  $\lambda = 2$  when gauge-fluctuations are suppressed, as is the case in the uniformly frustrated  $3DXY$ -model. Under such circumstances, the induction  $B$  will not acquire anomalous scaling. Hence, we obtain

$$B^{\alpha/2\nu} \Delta C(t, B) = y^{\alpha/2\nu} \left[ \mathcal{G}_{\pm}(y) - \mathcal{G}_{\pm}(0) \right] \equiv \mathcal{H}_{\pm}(y), \quad (7)$$

where  $y = B|t|^{-2\nu}$ . We will use the above scaling form Eq. 7 to determine the width of the crossover region around the upper critical field, as a function of  $B$ . Note, however, that this scaling form is not specific to the  $3DXY$ -model. By plotting appropriate ratios of temperature- and field-derivatives of these scaling functions, one may extract directly the critical exponents of the system as the slopes of the quantities being plotted, see for instance the very detailed analysis of this by Schilling *et al.*<sup>16</sup>. It is conceivable that such a procedure would yield a curve with a kink in it when  $t > 0$ , as claimed to be observed by Schilling *et al.* This in itself does not invalidate the  $3DXY$ -scaling of high- $T_c$  cuprates. Conceivably, it could be due to a crossover from an  $XY$  fixed point to another fixed point, possibly with an anomalously large value of  $\nu \approx 1.5$ , based on magnetization data. (Note that the specific heat data of Schilling *et al.* in fact show an opposite trend, more consistent with a crossover to a Gaussian fixed point. This is to be expected if amplitude fluctuations of the order parameter were to dominate the phase-fluctuations). For more details, see the discussion below.

We note immediately that the above implies that  $|t| \sim B^{1/2\nu}$  for finite fields, i.e. the width of the crossover region widens as  $B$  increases. Using the estimate  $\nu = 2/3$

in three dimensions, we have  $|t| \sim B^{3/4}$ , implying that the crossover region around the upper critical on the low-temperature side has a positive curvature in the  $B - T$  phase-diagram, which is also true for the melting curve, for which we have  $|t|_M \sim B^{\eta}$ , with  $\eta \sim 2/3$ . The widening of the crossover region is of course consistent with a broadening of the remains of the zero-field anomaly in the specific heat, to be calculated below.

The crossover curve  $\tilde{B}(T < T_c)$  has a more rapid increase as a function of  $T_c - T$  than the melting curve, recall the exponents  $3/4$  and  $2/3$ , respectively. Due to the finite width of the zero-field critical region, there should then be a field regime where either the melting curve and the crossover curve intersect, or where the crossover curve is to the left of the melting curve in the  $B - T$  phase-diagram. This depends on the width of the zero-field critical regime. Given the size of this regime,  $|t| \leq 0.1$ , the former scenario appears to us to be the more likely one, and this is also what we find in our simulations. Hence critical fluctuations, i.e. thermally induced vortex loops, should substantially influence the FLL melting in a finite regime of magnetic fields. From our simulations, to be presented below, we estimate the relevant field regime to be of order  $0 - 1T$  in an extreme type-II superconductor with  $\Gamma = 3$ .

### C. The helicity modulus

As a probe of global superconducting phase-coherence, we consider various helicity moduli  $\Upsilon_x$ ,  $\Upsilon_y$  and  $\Upsilon_z$ . The helicity modulus  $\Upsilon_{\mu}$  along the  $\mu$ -direction is defined as the second derivative of the free energy with respect to a global phase twist along the  $\mu$ -direction<sup>19</sup>, explicitly we obtain for the anisotropic uniformly frustrated  $3DXY$ -model

$$\Upsilon_{\mu} = \frac{1}{L_{\perp}L_z} \left\langle \sum_{\mathbf{r}, \nu=x,y,z} J_{\nu} \cos[\nabla_{\nu}\theta(\mathbf{r}) - A_{\nu}(\mathbf{r})](\hat{e}_{\nu} \cdot \hat{e}_{\mu})^2 \right\rangle - \frac{1}{k_B T L_{\perp}L_z} \left\langle \left[ \sum_{\mathbf{r}, \nu=x,y,z} J_{\nu} \sin[\nabla_{\nu}\theta(\mathbf{r}) - A_{\nu}(\mathbf{r})](\hat{e}_{\nu} \cdot \hat{e}_{\mu}) \right]^2 \right\rangle.$$

When  $\Upsilon_{\mu}$  is finite, the system can carry a supercurrent along the  $\mu$ -direction. When  $\Upsilon_{\mu}$  vanishes, resistivity along the  $\mu$ -direction becomes finite. In systems with finite applied field along the  $z$ -axis, we expect  $\Upsilon_x = \Upsilon_y = 0$  for all temperatures in the continuum limit. In this case, any applied current along the  $xy$ -plane will move the unpinned flux lines and dissipate energy. Discretization introduces a potentially singular perturbation by introducing an artificial pinning potential, the effect of which is more serious in a three-dimensional system than in a two-dimensional one. In the latter case, the effect of the potential may in principle be entirely avoided by considering low enough filling fractions<sup>27</sup>, whereas this is not possible in three dimensions in the thermodynamic

limit. The size  $L_z$  of systems must therefore be tailored to the filling fraction  $f$  in order to avoid spurious pinning effects.

The thus introduced pinning potential will, at a low enough temperature, pin the flux lines in their positions, and cause  $(\Upsilon_x, \Upsilon_y) \neq 0$  up to a depinning temperature  $T_d$ . To ensure that this artificially introduced pinning potential caused by the numerical lattice does not affect the FLL melting transition, we should consider systems with  $T_d$  much lower than all other ‘‘critical’’ temperatures of interest.  $T_d$  is controlled mainly by the filling fraction  $f$ ; we have  $T_d \rightarrow 0$  as  $f \rightarrow 0$ <sup>27,9</sup>. To adequately mimick the continuum limit of interest, low enough filling fractions must therefore be considered.

#### D. The FLL structure function

To locate the position of the vortex elements we use the following procedure: The counterclockwise line integral of the gauge-invariant phase-differences around any plaquette of the numerical lattice with surface normal along the  $\mu$ -direction must always satisfy

$$\sum_{C_i} j_\nu(\mathbf{r}) = 2\pi(n_\mu(\mathbf{r}) - f_\mu),$$

$$j_\nu(\mathbf{r}) = \nabla_\nu \theta(\mathbf{r}) - A_\nu(\mathbf{r}).$$

Here,  $C_i$  is the closed path traced out by the links surrounding an arbitrary plaquette, and  $\nu$  represents the Cartesian components of the current in the directions of the links which comprise the closed path  $C_i$ . Furthermore,  $j_\nu(\mathbf{r})$  is the current on the link between site  $\mathbf{r}$  and site  $\mathbf{r} + \hat{e}_\nu$ , and  $n_\mu(\mathbf{r}) = 0, \pm 1$  represents a vortex segment penetrating the plaquette enclosed by the path  $C_i$ . Here,  $f_\mu$  is the vortex lines density along the  $\mu$ -direction, and is given by

$$f_\mu = \frac{\sum_{\vec{r}} n_\mu(\vec{r})}{L_\perp L_z}. \quad (8)$$

To probe the structural order of the vortex-system, we consider the inplane structure function for  $n_z$  vortex segments within the same plane<sup>2</sup>,

$$S(\mathbf{k}_\perp) = \frac{1}{f^2 L_\perp^2 L_z} \left\langle \sum_z \left| \sum_{\mathbf{r}_\perp} n_z(\mathbf{r}_\perp, z) e^{i\mathbf{k}_\perp \cdot \mathbf{r}_\perp} \right|^2 \right\rangle.$$

In the FLL phase we expect to see a periodic array of sharp Bragg peaks in the  $\mathbf{k}_\perp$ -plane. In the vortex liquid phase we expect to see Bragg rings with radius  $k_\perp = 2\pi/a_v$  and  $4\pi/a_v$ , characteristic of a liquid. Here,  $a_v$  is the average distance between neighboring vortex lines.

#### E. Monte Carlo procedure

The Monte Carlo updating procedure used in this paper is the following. The numerical lattice is stepped through in a systematic manner. At each site a change of the local phase of the superconducting condensate is attempted by a random amount  $\Delta\theta \in [-\pi, \pi)$ . The attempt is accepted or rejected according to the standard Metropolis algorithm.

If the accepted phase change causes the current on a link  $j_\mu(\vec{r})$  to fall exceed the range  $j_\mu(\vec{r}) \in [-\pi, \pi)$ , an amount  $\pm 2\pi$  is added to the current such that  $j_\mu(\vec{r})$  is brought back into the primary interval  $j_\mu(\vec{r}) \in [-\pi, \pi)$ . An important point is that this operation can only generate a closed unit vortex loop around the link where the current is changed, thereby conserving the net induction of the system. No net vorticity is ever introduced by the procedure, and the procedure also guarantees that no vortex line can start or end within the sample. One sweep refers to  $L_\perp^2 L_z$  attempts to change the phase angle.

We fix the height of our systems to  $L_z = 40$  and let  $L_\perp$  vary from 40 to 128 depending on the flux-line density under consideration. In Refs.<sup>8,9</sup>, it was noted that for systems with moderate anisotropy ( $\Gamma \sim 3$ ), finite size effects are rather small when the linear dimension of the system and the total number of flux lines exceed  $\sim 40$ . Thus, we believe that finite size effects will not affect the conclusions in this paper. Likewise, it was observed by the same authors that finite-size effects were negligible when  $L_z$  was increased beyond  $L_z = 40$  for the anisotropy considered here,  $\Gamma = 3$ . This has motivated our choice of  $L_z = 40$ .

In this paper we fix the anisotropy parameter  $\Gamma$  to

$$\Gamma \equiv \sqrt{\frac{J_\perp}{J_z}} = \frac{\lambda_z d}{\lambda_{ab} \xi_{ab}} = 3.$$

in most simulations. Occasionally, comparison is made for the isotropic case  $\Gamma = 1$ . The magnetic field  $B$  is applied along the crystal  $c$ -axis, giving a vortex line density  $f$ ,

$$f_x = f_y = 0, \quad f_z \equiv f = \frac{B \xi_{ab}^2}{\Phi_0}. \quad (9)$$

The flux-line densities  $f$  considered are:  $1/f = 12$  (48), 14 (56), 16 (48), 20 (40), 25 (50), 32 (64), 48 (48), 64 (64), 72 (72), 84 (84), 96 (96), 112 (112), 128 (128),  $\infty$  (64). The numbers in the parentheses denote  $L_\perp$  for the corresponding vortex line density. Note that we have chosen, with our gauge,  $L_\perp$  for each filling fraction  $f$  in such a way that we ensure that an integer number of magnetic Brillouin-zones will fit on the reciprocal lattice of each system, enabling us to use periodic boundary conditions in the  $x, y$ -directions. As will be observed,  $L_\perp$  is an integer number of  $1/f$  in each case.

The value of  $f$  is prescribed by loading the following phase-difference pattern onto the numerical lattice (using Landau gauge) a system with  $\theta(\mathbf{r}) = 0$  for all  $\mathbf{r}$ ,

$$A_y(x, y, z) = 2\pi f x.$$

The system is then heated to a temperature well above any transition/crossover temperatures of interest, at which point slow cooling is started. The filling fraction  $f$  is conserved by our Monte Carlo procedure, and the moves are carried out on the gauge-invariant phase-differences on each link. Note that we do not need to *assume* any ground state configuration by this procedure. Extremely long simulations, typically  $4 \times 10^6 - 6 \times 10^6$  sweeps, are however required in order to capture the correct physics at the FLL melting transition and to reveal any  $\delta$ -function anomalies in the specific heat at the melting transition, particularly at low filling fractions.

### III. RESULTS, $F = 1/20$

#### A. FLL melting and phase-coherence

To identify the possible different phases and phase transition(s)/crossover(s) in a system with finite flux-line density, we first concentrate on results for the system  $f = 1/20$ . *Similar results are found in all other finite flux-line densities considered in this paper*, to be detailed below. We have measured temperatures in units where  $k_B = 1$ .

Fig. 1 shows the specific heat per site  $C$ , the helicity modulus along the applied field direction  $\Upsilon_z$ , the helicity modulus perpendicular to the applied field direction  $\Upsilon_x$ , and the inplane structure function  $S(\mathbf{k}_\perp)$ , as functions of temperature. Fig. 1 shows that the inplane structure function  $S(\mathbf{k}_\perp = 2\pi/5, \pi/4)$  has a sharp drop from 0.2 to 0 precisely at  $T_m = 0.531J_\perp$ , indicating that the FLL melts at  $T_m$  in a first order phase transition. For a more global view, Fig. 2 illustrates the density plot of  $S(\mathbf{k}_\perp)$  for  $k_x, k_y \in [-\pi, \pi]$  at four different temperatures;  $T/J_\perp = 0.450, 0.530, 0.531, 0.532$ . It is clearly seen that the periodic array of sharp Bragg-peaks is converted into a ring precisely at  $T_m = 0.531J_\perp$ , within a narrow temperature region of  $\Delta T = 0.001J_\perp$  around  $T_m$ .

To clarify whether the phase coherence along the direction of the applied magnetic field is finite in the vortex liquid phase, we consider the helicity modulus along  $z$ -axis,  $\Upsilon_z$ . In Fig.1 it is clearly seen that  $\Upsilon_z$  shows a sharp jump from 0.6 to 0 at  $T_m$  precisely where the FLL melts. This shows that the FLL melts directly into an *incoherent vortex liquid* in a first order phase transition. We will return to this important point later, since it has important consequences for the physical picture of the vortex liquid phase. The above result is in complete agreement with the work of Ref.<sup>8</sup> using the  $3DXY$ -model, the work of Ref.<sup>22</sup> using the lowest Landau-level approximation, and earlier work by us using the  $3D$  anisotropic Villain model<sup>9</sup>. In all these works, it was found that longitudinal phase-coherence is lost as soon as the vortex lattice melts in the thermodynamic limit. We emphasize that opposite conclusions were drawn in earlier work by us

and others<sup>7,19,29</sup>. We believe that this discrepancy may be due to one or several of the following three factors: i) In earlier work, the system size in the  $z$ -direction may not have been large enough, particularly for the isotropic case, ii) the simulations were not run for a long enough time, and iii) the results were obtained upon heating only. Our more recent results in Ref.<sup>9</sup> and in the present paper are obtained upon heating *and* cooling.

A first order phase transition is manifest in the form of a  $\delta$ -function anomaly in the specific heat. From the height of this anomaly one may deduce the latent heat of the transition. Fig.1 shows that the anomaly occurs at  $T_m = 0.531J_\perp$ , precisely where the structure function and the helicity modulus vanish. These results are in complete agreement with those of Refs.<sup>8</sup> obtained on the uniformly frustrated  $3DXY$ -model for  $f = 1/25$ , as well as those found in Ref.<sup>9</sup> using the uniformly frustrated  $3D$  anisotropic Villain-model for  $f = 1/32$ . Below we consider filling fractions down to  $f = 1/128$ , finding that these results still hold.

The latent heat of the first order FLL melting transition at  $T_m$  is obtained from the jump in the internal energy shown in Fig. 3, using Eq. 4. Here, the entropy jump per vortex line per layer is estimated to be  $\Delta S = 0.1k_B$ . To obtain the spike in the specific heat we must i) find the transition temperature must be located very accurately, typically to within a part in  $10^3$  and ii) increase the simulation length to at least 6000000 sweeps over the lattice for each temperature. The extreme length of the simulations is necessary to allow the system to switch back and forth between the ordered phase and disordered phase at the phase transition an adequate number of times, typically at least ten times.

#### B. Breakdown of the 2D boson analogy

The specific heat has a broad anomaly at  $T_{Bc2} \simeq 1.05J_\perp \gg T_m$ , indicating a crossover. This broad crossover was unambiguously identified in our previous work as the remains of a zero field Onsager vortex loop “blow out”<sup>7,9</sup>, destroying superconductivity on all length scales. However, since the remains of the zero field vortex loop “blow out” takes place first at  $T_{Bc2} \gg T_m$ , superconductivity still exists locally in finite domains in the incoherent vortex liquid phase, giving strong diamagnetic fluctuations<sup>20</sup>. Since the global phase coherence in all directions is destroyed in the incoherent vortex liquid phase, the superfluid stiffness is zero in all directions in this phase, and any applied current through the system will dissipate energy. Thus, in the incoherent vortex liquid phase the system has both finite resistivity in all directions, as well as strong diamagnetic fluctuations. The numerical lattice is a singular perturbation in a three dimensional system, and one may ask whether the first order FLL melting transition at  $T_m$  is affected by the artificially introduced pinning potential. To address this

issue we consider the helicity modulus along the x-axis,  $\Upsilon_x$ . In Fig. 1, it is seen that the helicity modulus along x-axis  $\Upsilon_x$  drops to zero already at  $T_d = 0.1J_\perp \ll T_m$ . From this we conclude that above  $T_d$  the system exhibits a “floating solid” phase<sup>27</sup>. Thus the FLL melting transition at  $T_m$  is *not* affected by the pinning potential caused by the numerical lattice.

Snapshots of the FLL, the incoherent vortex liquid phase, and the normal metal phase are shown in Fig. 4, of the system  $f = 1/20$  for four temperatures  $T/J_\perp = 0.26, 0.50, 0.54, 0.70$ . For clarity only a part of the system;  $x, y \in [0 : 20], z \in [0 : 40]$ , is shown. For the system  $f = 1/20$ , we have found  $T_m = 0.53J_\perp$  and  $T_{Bc2} = 1.05J_\perp$ . For  $T = 0.26J_\perp \ll T_m$ , the flux lines form a hexagonal lattice. Although there are many thermally induced defects attached to each flux line, they remain well defined entities. For  $T = 0.50J_\perp \lesssim T_m$ , though the flux lines now fluctuate substantially, they nonetheless remain intact. So does the FLL, as evidenced by the results for the structure function, see Figs. 1 and 5. For a slightly more elevated temperature  $T = 0.54J_\perp \gtrsim T_m$ , the FLL has melted. A key observation is that, immediately upon melting, the flux lines are no longer well defined entities, there are many intersections between flux lines, vortex-loops have proliferated, and there exists at least one way to percolate from one side of the sample to the opposite side in any direction. Thus, for any given direction there always exist at least one “infinite” long vortex lines perpendicular to it, and any applied current will move these “perpendicular” vortex lines and dissipate energy. Note that in this picture vortex lines in the incoherent vortex liquid cannot be described as world lines of *2D non-relativistic bosons*<sup>2</sup>. Thus, one vortex line in the center of the system will meander all the way to the boundary surface (with surface normal perpendicular the applied field direction) and back as a field induced flux line weaves its way from the bottom to the top of the system. This corresponds to zero flux-line tension, and a wandering exponent  $\zeta$  of the flux line which is  $\zeta \geq 1$  or, equivalently, zero bosonic mass in the *2D boson* analogy.

Note that the *2D quantum boson* system we have in mind when referring to the work of Ref.<sup>2</sup> is a non-relativistic system. The picture we have in mind for the liquid phase is more akin to a *relativistic 2D quantum boson* system, where the proliferation of vortex loops and overhangs in the flux-lines correspond to vacuum-fluctuations in the boson system. This connection has been nicely exposed in Ref.<sup>28</sup>.

## IV. RESULTS, $1/F \in [12, \dots, 128]$

### A. Structure function $S(\mathbf{k}_\perp)$

We show in Fig. 5 the inplane structure function  $S(\mathbf{k}_\perp)$  as a function of temperature for several vortex line den-

sities  $f$ ;

$1/f = 12(\mathbf{k}_\perp = 5\pi/12, 5\pi/12), 16(\mathbf{k}_\perp = 3\pi/8, -\pi/3), 20(\mathbf{k}_\perp = 2\pi/5, \pi/4), 25(\mathbf{k}_\perp = 6\pi/25, 9\pi/25), 32(\mathbf{k}_\perp = 5\pi/16, -7\pi/32), 48(\mathbf{k}_\perp = \pi/6, \pi/4), 72(\mathbf{k}_\perp = \pi/9, -2\pi/9), 96(\mathbf{k}_\perp = 3\pi/16, 5\pi/58), 128(\mathbf{k}_\perp = 7\pi/64, 5\pi/32)$ . For a given vortex line density,  $S(\mathbf{k}_\perp)$  with the corresponding value of  $\mathbf{k}_\perp$  shows a sharp drop from  $\sim 0.2$  to zero defining a field dependent FLL melting temperature  $T_m(f)$ . This clearly shows that, for all values of  $f$  considered here, the FLL melts in a first order phase transition. For decreasing  $f$ , the transition temperature  $T_m(f)$  increase towards  $T_c$  as expected, see Fig. 7.

### B. Helicity modulus along the field direction, $\Upsilon_z$

In Fig. 6 the helicity modulus  $\Upsilon_z$  along the direction of the magnetic field is shown as a function of temperature for the same set of flux-line densities as for the case of the inplane structure function. As  $f$  is varied,  $\Upsilon_z$  shows a sharp drop towards zero precisely at the corresponding FLL melting temperature  $T_m(f)$ . Thus, we may conclude that for all filling fractions considered, the FLL melts directly into an incoherent vortex liquid. The temperature region where the vortex liquid and the phase coherence along the applied field coexist, found previously by several authors<sup>19,20,7,12</sup>, is not found for any flux-line density  $f$  considered in this paper. We believe that the temperature regime where the vortex liquid exist with phase coherence along the field direction pertains to thin film geometries, or are otherwise an artifact too short simulations and hysteretic behavior in the heating/cooling sequence of the vortex system. The phase-coherent vortex liquid does not exist in the thermodynamic limit of an equilibrium system, at least in systems with moderate anisotropy and moderate magnetic induction. The possibility of the existence of a very small magnetic field induction  $B_{lower}$  (dependent on the anisotropy  $B_{lower}(\Gamma)$ ) below which the phase coherence along the field direction can exist in the vortex liquid is not completely ruled out by this work.

Note that  $T_m(f)$  is correlated with the temperature where the corresponding  $\Upsilon_z$  start to fall sharply towards zero, not the lowest temperature where  $\Upsilon_z$  vanish. One may question whether it is correct to take the temperature where  $\Upsilon_z$  starts to show a sharp drop as the temperature where phase coherence along the applied field vanish. For moderate vortex line densities this poses no problem, since the drop in  $\Upsilon_z$  is very sharp. However, for  $f < 1/48$ , the transition extend over a small temperature region. By experience, we know that when the system size and the number of vortex lines in the system increases, the drop in  $\Upsilon_z$  sharpens and the tail in  $\Upsilon_z$  disappear. We believe therefore that this tail is only a finite size effect.

The main conclusion of the above discussion is that in the thermodynamic limit, no phase-coherence exists in

the vortex liquid phase. This conclusion is consistent with mounting evidence from numerical simulations<sup>8,9,30</sup>, obtained however only in a limited filling range  $1/f \in [25 - 36]$ . Our present results extend these conclusion to much lower filling fractions.

### C. Specific Heat

For all filling fractions down to  $f = 1/32$ , we have found a  $\delta$ -function anomaly in the specific heat at  $T_m(f)$ , indicating a first order phase transition, see Fig 7. For smaller filling fractions  $f \leq 1/48$  we find no clear evidence of a spike in the specific heat. Note that in passing from the system with  $f = 1/32$  to the system with  $f = 1/48$ , the number of field induced flux lines is reduced from 128 to 48. We believe that the observed “none-existence” of the  $\delta$ -function anomalies at the FLL melting temperature in system with very low flux-line densities is attributable to two factors: 1) for system with  $f \leq 1/48$  we have to few field induced vortex lines in our systems, and 2) the contribution to the specific heat from the field induced flux lines for these filling fractions is too small compared to the “spin-wave” and vortex-loop contributions, to be detected by our simulations.

In Fig. 8, we show the specific heat as a function of temperature for the same set of corresponding system sizes and flux-line densities as previously used in calculating the inplane structure function and the helicity modulus along the direction of the applied magnetic field. For decreasing  $f$  the crossover temperature  $T_{BC2}(f)$  increases and moves towards the zero-field critical temperature  $T_{BC2}(f = 0) = T_c$ . The broad anomaly in the specific heat sharpens and the maximum height of the cusp increases, evolving smoothly towards the zero-field specific heat singularity at  $T_c$ .  $T_{BC2}$  denotes the crossover temperature at which the remains of the zero field vortex-loop “blowout” takes place. In a finite magnetic field the vortex -loop “blowout” at  $T_{BC2}(f)$  causes only a crossover and the actual phase transition takes place at a lower temperature,  $T_m(f)$ , where the FLL undergoes a first order melting transition triggered by a proliferation of vortex loops with diameters at least of order the magnetic length in the problem.

Scaling functions for the specific heat both for zero field and finite field are shown in Figs. 9 and 10. For the zero-field case, using Eq. 6, it is seen from Fig. 9 that data-collapse is obtained over a wide region out to values of the scaling variable  $|t|L^{1/\nu} > 10$  for  $L \geq 32$  on the low-temperature side of  $T_c$ . Note also that the width of the scaling regime is slightly larger for  $\Gamma = 3$  than for  $\Gamma = 1$ . We expect this trend to persist with increasing  $\Gamma$ ; in the extremely case where the layers may be considered completely decoupled, i.e.  $\Gamma \rightarrow \infty$ , the

entire low-temperature regime is known to be critical<sup>31</sup>. For smaller  $L$ , it appears from our simulations that we do not obtain scaling. Using the value  $\nu = 0.669$ <sup>26</sup>, we find that the width of the critical region is given by  $|t| \approx 0.1$ . The critical scaling of the specific heat is also considerably better above  $T_c$  than below. This is due to the fact that vortex loops, i.e. the critical fluctuations, to a much larger extent dominate the free energy above  $T_c$  compared to below  $T_c$ . Below  $T_c$  there is a non-singular contribution to the free energy, and hence specific heat, due to spin-wave fluctuations of the local phase of the order parameter.

The scaling function of the specific heat in a finite field, given above in Eq. 7, is also calculated for filling fractions  $f$  given by  $1/f = 12, 16, 20, 25, 32, 48, 72, 96, 128$  with corresponding system sizes identical to those used for the structure function above. The anisotropy is  $\Gamma = 3$ . The scaled results are good agreement with the works of Salamon *et al.*<sup>13</sup>, Roulin *et al.*<sup>14</sup>, and Schilling *et al.*<sup>16</sup>. Note that while Ref.<sup>16</sup> makes the point that  $3DXY$ -scaling does not appear to describe well the experimental results above  $T_c$  in a single-crystal  $YBa_2Cu_3O_7$  in the field-range  $0.75 - 7T$ , it does appear to work well below  $T_c$ . The reason for this may be that for an optimally doped compound, the temperature at which a pseudo-gap opens up may not be much higher than  $T_c$  at which phase-coherence is established. The results are therefore likely to be influenced by amplitude fluctuations above  $T_c$ . This should not be the case below  $T_c$ . Hence, we believe that the field range considered is not the only issue, but also that one is observing a crossover from an XY-critical point to a Gaussian critical point when increasing the temperature above  $T_c$ , approaching a mean-field like temperature  $T_{MF}$  where preformed pairs start to be dissociate. An obscuring factor is that the specific heat data and magnetization data of Schilling *et al.* show opposite trends in their deviation from XY-scaling. Note that the analysis of Ref.<sup>16</sup> is *not* specific to the XY-model, the scaling forms that are used are quite general. Were the temperature scales  $T_c$  and  $T_{MF}$  to be well separated, XY critical scaling would presumably persist above  $T_c$ . This would for instance be the case in *underdoped* cuprates<sup>32</sup>. At any rate, it is the width of the critical region *below*  $T_c$  which is of interest in establishing the importance of interplay between vortex loops and FLL melting. The width of the critical region should increase with underdoping, and hence the interplay between vortex loops and FLL melting is expected to be more pronounced when the cuprates become more underdoped<sup>32</sup>. We note that the scaling is better above  $T_c$  than below, again because non-singular contributions to the free energy, in this case also arising from the FLL, contribute significantly. The spikes in the finite-field scaling function are due to the specific heat anomalies at the FLL melting transition.



### D. Entropy discontinuity at the FLL melting transition

The latent heat, or equivalently the discontinuity in entropy at the FLL melting transition, has been much focused on in recent experiments<sup>33,34,11,15,14</sup>. In Fig.11, the entropy discontinuity at the first order FLL melting transition is shown as a function of the flux-line density. The results obtained using the Hamiltonian in Eq. 1 is shown in filled circles. We find that the entropy discontinuity per flux line per layer  $\Delta S(f) \sim 0.1k_B$ . The fact that  $\Delta S$  is essentially independent of the applied magnetic field, *for the moderate anisotropy*  $\Gamma = 3$  considered in this paper, is consistent with the experimental results obtained by Schilling et al.<sup>15</sup> and Roulin et al.<sup>14</sup>. They found  $\Delta S(B) \sim 0.5k_B$ , independent of  $B$ . The values of  $\Delta S = 0.1k_B$  are similar to the values found by Hu et al.<sup>8</sup>. We attribute the difference between our values for  $\Delta S(f) \sim 0.1k_B$  and the experimental value  $\Delta S(B) \sim 0.5k_B$  to the difference in the anisotropy. YBCO has an anisotropy  $\Gamma \sim 7$ , while the anisotropy in this paper is  $\Gamma = 3$ . As shown in our previous paper<sup>9</sup>, and also by Hu et al.<sup>8</sup>, the entropy jump at the FLL melting transition increases with increasing anisotropy.

To ensure that the artificial pinning potential introduced by the numerical mesh does not affect the FLL melting transition at  $T_m(f)$ , we must ensure that the helicity modulus perpendicular to the applied field vanishes at a temperature  $T_d(f)$  significantly below  $T_m(f)$ . Under such circumstances, the low temperature phase for  $T_d(f) < T < T_m(f)$  is characterized by a “floating solid phase”, mimicking the continuum limit. In Fig. 12, the helicity modulus along x-direction  $\Upsilon_x$  is shown as a function of temperature for the same set of  $f$  used for the specific heat, structure function, and  $\Upsilon_z$ . Fig. 12 shows that for each flux-line density considered,  $\Upsilon_x$  vanishes at a temperature  $T_d(f)$  significantly lower than the corresponding FLL melting temperature  $T_m(f)$ . Thus, we have shown that in all systems considered in this paper, the depinning crossover at  $T_d(f)$  does not affect the FLL melting at  $T_m(f) \gg T_d(f)$ . Although we have not shown it explicitly here, we have checked that  $\Upsilon_y(T)$  is essentially identical to  $\Upsilon_x$ , as required by symmetry.

In recent work<sup>35</sup>, it was pointed out that calculated entropy jumps  $\Delta S$  at the melting transition of the Abrikosov vortex lattice could be brought into agreement with experiments<sup>15</sup> by introducing temperature dependent parameters in the theory, reflecting fluctuations at a microscopic level surfacing in coarse grained theories. The idea of using such a procedure was first introduced by in Ref.<sup>22</sup> within the lowest Landau level approach to the same problem, i.e. the high-field limit. This leads to an internal energy

$$U(T) = \langle H \rangle - T \left\langle \frac{\partial H}{\partial T} \right\rangle, \quad (10)$$

where  $H$  is an effective  $T$ -dependent Hamiltonian,

$\langle H \rangle = (1/Z) \sum H \exp(-H/k_B T)$ , and  $Z = \sum \exp(-H/k_B T)$  is the canonical partition function. For a derivation of this result, see Appendix A.

In extreme type-II superconductors, as modelled by the  $3DXY$ -model or the London model in the  $\lambda \rightarrow \infty$ -limit, the  $T$ -dependence described above appears exclusively as a prefactor in the Hamiltonian,  $H = E_0(\tau)H_0$ , where  $H_0$  has no  $T$ -dependent prefactors,  $\tau = T/T_{cMF}$  with  $T_{cMF}$  a mean-field zero-field transition temperature, and  $E_0(\tau) = [\lambda(0)/\lambda(\tau)]^2$ .  $H_0$  is to be identified with the Hamiltonian used in this paper so far. For instance, in the two-fluid model  $E_0(\tau) = 1 - \tau^2$ , while the simplest mean-field approximation yields  $E_0(\tau) = 1 - \tau$ . Using the above, we find the internal energy given by

$$\begin{aligned} U &= \left[ E_0(\tau) - T \frac{dE_0(\tau)}{dT} \right] U_0(T'), \\ U_0(T') &= \frac{1}{Z} \sum H_0 \exp(-H_0/k_B T'), \\ T' &= \frac{T}{E_0(\tau)}. \end{aligned} \quad (11)$$

This leads to an entropy jump at the first-order melting transition of the Abrikosov vortex lattice

$$\begin{aligned} \Delta S &= \frac{\Delta U}{T} = \left[ E_0(\tau) - T \frac{dE_0(\tau)}{dT} \right] \frac{\Delta U_0(T')}{T} \\ &= \frac{1}{E_0(\tau)} \left[ E_0(\tau) - T \frac{dE_0(\tau)}{dT} \right] \Delta S_0(T'), \end{aligned} \quad (12)$$

where  $\Delta S_0(T') = \Delta U_0(T')/T'$  is the entropy jump obtained without any  $T$ -dependent parameters in the Hamiltonian, but where the quantity is to be evaluated at the temperature  $T' = T/E_0(\tau)$ . Note that the prefactor relating  $\Delta S$  to  $\Delta S_0$  would always be 1 irrespective of what  $E_0(\tau)$  is, if we had not included the contribution  $-T < \partial H / \partial T >$  to  $U$ . Using  $E_0(\tau) = 1 - \tau^2$ , we find

$$\Delta S(T) = \frac{1 + \tau^2}{1 - \tau^2} \Delta S_0(T'), \quad (13)$$

precisely as in Ref.<sup>35</sup>. Note the difference in the arguments of  $\Delta S(T)$  and  $\Delta S_0(T')$ . Ref.<sup>35</sup> concludes that within a line-liquid model with moderate values of  $\Delta S_0$ , substantially enhanced values for  $\Delta S$  are obtained, particularly in the low-field regime, in agreement with experiments. The main factor in the enhancement is the denominator  $1 - \tau^2$ , which vanishes as  $T \rightarrow T_{cMF}$ .

Note that the above procedure of substituting  $H_0$  with  $E_0(\tau) H_0$  does not in itself in any way assume that the physics of the vortex system in the low-field regime is determined exclusively by field-induced flux lines. However, were we to follow Ref.<sup>35</sup> and in addition assume that in the low-field regime, there only exists one relevant length scale in the problem, namely the magnetic length  $a_0 \sim 1/\sqrt{B}$ , we would be assuming that only field-induced vortices are relevant degrees of freedom on the

melting line. Our main point is that this may be questionable in the low-field regime, and we will therefore refrain from utilizing such an assumption.

If we insist on comparing  $\Delta S_0(T')$  with results obtained using  $H_0$ , and not  $H^{35}$ , then we must fix  $T'$  to values obtained for the melting line in such calculations. Thus,  $\tau$  cannot vary arbitrarily between 0 and 1, while fixing  $\Delta S_0$  independently. Rather,  $\tau$  and  $T'$  are related via  $T' = T/E_0(\tau)$ . In calculations of  $\Delta S_0$  using  $H_0$ , we must therefore have  $T'/T_{CMF} < 1$ . Using  $E_0(\tau) = 1 - \tau^2$ , we find  $\tau < (\sqrt{5} - 1)/2$ . This gives enhancement factors  $(1 + \tau^2)/(1 - \tau^2) < \sqrt{5}$  within the two-fluid model. If we express Eq. 13 in terms of  $\tau' = T'/T_c$ , we obtain

$$\Delta S = \sqrt{1 + 4\tau'^2} \Delta S_0(T'); \quad \tau' \in [0, 1 > . \quad (14)$$

Similar enhancement factors may be found using the simplest mean-field approximation  $E_0(\tau) = 1 - \tau$ , as for instance used in Ref.<sup>30</sup>. It would yield an enhancement factor in Eq. 14 given by  $1 + \tau'$ . In Fig. 11 we have also plotted the entropy jump as obtained using a  $T$ -dependent prefactor in the Hamiltonian. We have used the results obtained using  $H_0$  and enhanced them by the prefactor in Eq. 14. The inset of the figure shows the enhancement factor on the melting line obtained in our simulations. It varies quite slowly as a function of  $\tau'$  in the entire interval. Hence, even if we include the effect of  $E_0(\tau)$  on  $\Delta S$ , we obtain an essentially field-independent entropy jump in the field regime considered in Fig. 11. For specificity, we have chosen  $E_0(\tau) = 1 - \tau^2$ , and ignored the difference between  $T_c$  and the mean-field critical temperature. We note also in this context that Ref.<sup>22</sup> finds an entropy jump of the magnitude we have found here within the lowest Landau-level approximation. Furthermore, Ref.<sup>29</sup> finds similar results using the isotropic  $XY$ -model with  $f = 1/6$ , in agreement earlier simulations on the same filling fraction<sup>18</sup>. Note the large difference in filling fractions between the present work and the work of Refs.<sup>29,18</sup>. For  $f = 1/6$ , commensuration effects due to the numerical lattice are severe, and could conceivably lead to overestimates of the magnitude of  $\Delta S$ . This has been part of the motivation for pushing the simulations to the low filling fractions used in this paper.

### E. B-T Phase Diagram

To estimate the real magnetic field induction  $B$  corresponding to the flux-line densities considered in this paper, we use Eq.8 and take  $\xi_{ab} = 12 - 15 \text{ \AA}$ . With this value of  $\xi_{ab}$ , we find the magnetic field corresponding to the smallest flux-line densities considered ( $f=1/128$ ) to be approximate  $5 - 7T$ . In Fig. 13 we show the f-T phase diagram originating from simulations of the  $XY$  model. The flux-line densities  $f$  considered are  $1/f = 12, 14, 16, 20, 25, 32, 48, 64, 72, 84, 96, 112, 128$ . We see that the overall behavior of this phase diagram is consistent with the phase diagram in YBCO measured by

Schilling *et al.*<sup>15</sup>, and Junod *et al.*<sup>14</sup>. The FLL melting line at  $T_m(f)$  separates the superconducting Abrikosov FLL phase from the incoherent vortex liquid phase, the latter being characterized by finite resistivity and strong diamagnetic fluctuations, with simultaneous loss of Bragg peaks in the FLL structure factor, flux-line integrity, and global phase-coherence in all directions. The remains of the zero field vortex loop “blow out” around  $T_{Bc2}(f)$  destroys phase-coherence on all length scales, and thus separates the incoherent vortex liquid phase from the normal metal phase. The melting line  $T_m(f)$  decreases with decreasing  $f$  with a positive curvature. Note also that the width of the critical region is large enough to influence the FLL melting transition over a sizeable field range. This field range is seen to extend up to  $f \approx 1/256$  which we may conservatively estimate to be at least of order  $0 - 1T$ .

## V. CONCLUSION

In this paper, we have investigated characteristics of the molten phase of the Abrikosov flux-line lattice via Monte-Carlo simulations on the three-dimensional uniformly frustrated  $XY$ -model. Bragg-peaks in the static structure factor and phase-coherence along the direction of the applied magnetic field are both lost simultaneously, rendering the vortex liquid phase-incoherent. This behavior is triggered by thermal excitations of closed vortex loops of diameters of the order of the average distance between flux lines in the low-temperature lattice phase. On the melting line, this mechanism suffices to produce highly nontrivial vortex configurations with appreciable statistical weight *on the template of field induced vortices*. These configurations are characterized by a “percolation” of closed vortex-loops threading the entire sample in any direction. In particular, this is the case for directions transverse to the direction of the applied magnetic field, which is tantamount to a loss of line tension of the field-induced flux lines. It renders a picture of the molten phase of the flux-line lattice in terms of a liquid of well-defined, separated, and directed line-objects, invalid. Equivalently, a picture in terms of world-lines of  $2D$  non-relativistic superfluid bosons is invalid in the liquid phase. An effective theory of the flux-line lattice melting and the vortex-liquid phase thus appears to present a formidable challenge involving the solution of a self-consistent coupled theory of field-induced flux-line objects, and thermally induced closed vortex-loops<sup>6-8</sup>. This coupling must evidently render the flux-line tension equal to zero in the liquid phase. Unfortunately, it is therefore doubtful that the intuitively appealing physics of directed polymers is particularly relevant for the vortex liquid phase.

Scaling functions for the specific heat are calculated, both in zero and finite magnetic field. The zero-field results yield a sizeable critical region  $|T - T_c|/T_c \approx 0.1$ , corrob-

orating the notion that critical fluctuations of extreme type-II superconductors, i.e. vortex loops, will influence such phenomena as flux-line lattice melting over an appreciable range of magnetic inductions, possibly up to fields of order  $1T$  in moderately anisotropic superconductors. The field range will depend on mass-anisotropy, since the width of the critical region and the low-field shape of the melting curve both appear to be influenced by the layeredness of the superconductor.

The finite-field results for the scaling functions for the specific heat, as well as the obtained phase-diagram for an anisotropy parameter  $\Gamma = 3$ , are consistent with experiments on the slightly more anisotropic cuprate high- $T_c$  superconductor YBCO, with  $\Gamma \approx 7$ .

Finally, we note that columnar defects will not be particularly efficient in enhancing the critical current density in a superconductor where the FLL melting line is strongly influenced by thermally excited closed vortex loops. (The influence of columnar defects on the vortex-system was studied using Monte-Carlo simulations in Ref.<sup>37</sup> for a filling fraction  $f = 1/2$ ). The vortex-loop susceptibility should be sensitive to the phase-stiffness of the superconductor. The phase-stiffness is in turn largely controlled by the superfluid density, and therefore also by the charge-carrier density. In order to avoid the detrimental effects on transport properties in high- $T_c$  superconductors from a vortex-loop “blowout”, an increase of the charge-carrier density appears to be essential.

## VI. ACKNOWLEDGMENTS

Support from the Research Council of Norway (Norges Forskningsråd) under Grants No. 110566/410, No. 110569/410, as well as a grant for computing time under the Program for Super-computing, is gratefully acknowledged. We thank S.-K. Chin, A. Hansen, J. S. Høye, A. E. Koshelev, and Z. Tešanović for discussions. J. Amundsen is acknowledged for assistance in optimizing our computer codes for use on the Cray T3E.

## APPENDIX A: INTERNAL ENERGY

In this appendix, we give a brief derivation of a generalized expression for the internal energy of a system with an effective  $T$ -dependent Hamiltonian. Consider a system in the canonical ensemble. For illustration, we will consider the well-known  $(P, V, T)$ -system. Our result for the internal energy  $U$  does not depend on the nature of the work-term. The system has a statistical distribution function given by the canonical law

$$\rho = \frac{1}{Z} e^{-\frac{H}{\theta}}, \quad (\text{A1})$$

where the normalization constant  $Z$  is the canonical partition function

$$Z = \sum_{\text{configurations}} e^{-\frac{H}{\theta}}, \quad (\text{A2})$$

where  $\theta$  is a parameter of the distribution function which remains to be determined, such that

$$\sum_{\text{configurations}} \rho = 1. \quad (\text{A3})$$

We insist that this normalization is to be maintained if the parameters  $V$  and  $\theta$  are varied differentially. The Hamiltonian and hence the partition function will depend on  $V$  through the wall-potential of the problem. Let us, arbitrarily, write the partition function in the following way

$$Z = e^{-\frac{\Psi}{\theta}}, \quad (\text{A4})$$

where  $\Psi$  is a system-dependent parameter which also remains to be determined. When  $V \rightarrow V + dV$  and  $\theta \rightarrow \theta + d\theta$ , we will therefore also need to vary  $\Psi \rightarrow \Psi + d\Psi$  in order to maintain correct normalization of  $\rho$ . Hence, we have

$$\sum e^{\frac{\Psi - H(V, \theta)}{\theta}} = 1 = \sum e^{\frac{\Psi + d\Psi - H(V + dV, \theta + d\theta)}{\theta + d\theta}}. \quad (\text{A5})$$

Note that we have allowed  $H$  to depend on the statistical parameter  $\theta$ . Expanding to first order in all differentials, we obtain

$$\sum e^{\frac{\Psi - H(V, \theta)}{\theta}} \left[ 1 + \frac{1}{\theta} \left( d\Psi - \left( \frac{\partial H}{\partial V} dV + \frac{\partial H}{\partial \theta} d\theta \right) - \frac{d\theta}{\theta} (\Psi - H) \right) \right] = 1. \quad (\text{A6})$$

Since the original distribution prior to changing  $V \rightarrow V + dV$  and  $\theta \rightarrow \theta + d\theta$  also was normalized we obtain the following constraint on the differentials  $dV$ ,  $d\theta$ , and  $d\Psi$

$$d\Psi = \frac{d\theta}{\theta} [\Psi - \langle H \rangle + \theta \langle \frac{\partial H}{\partial \theta} \rangle] + \langle \frac{\partial H}{\partial V} \rangle dV. \quad (\text{A7})$$

Here,  $\langle \dots \rangle$  denotes a statistical average with respect to the original distribution function  $\exp((\Psi - H)/\theta)$ . In order to make the connection to thermodynamics, we now compare the above with the “thermodynamic identity”

$$dF = -S dT - P dV = \frac{dT}{T} (F - U) - P dV, \quad (\text{A8})$$

where  $F = U - TS$  is Helmholtz free energy,  $S$  is the entropy, and  $U$  is the internal energy. This comparison yields directly

$$\begin{aligned} P &= \left\langle -\frac{\partial H}{\partial V} \right\rangle, \\ \frac{d\theta}{\theta} &= \frac{dT}{T} \rightarrow \theta = k_B T, \\ \Psi &= F \\ U &= \langle H \rangle - T \left\langle \frac{\partial H}{\partial T} \right\rangle. \end{aligned} \quad (\text{A9})$$

Note that  $\Psi$  thus identified is the only choice consistent with  $F = -k_B T \ln Z$ . This then fixes  $U$ . Also, the expression for  $U$  obtained in this fashion is identical to that obtained directly from the usual relation

$$U = -\frac{\partial \ln Z}{\partial \beta}, \quad (\text{A10})$$

with an assumed  $T$ -dependent Hamiltonian.

- 
- <sup>1</sup> P. L. Gammel, D. J. Bishop, G. J. Dolan, J. R. Kwo, C. A. Murray, L. F. Schneemeyer, and J. V. Waszczak, Phys. Rev. Lett., **59**, 2592 (1987); *ibid*, **61**, 1666 (1988).
- <sup>2</sup> D. R. Nelson, Phys. Rev. Lett., **60**, 1973 (1988); D. R. Nelson and H. S. Seung, Phys. Rev. B **39**, 9153 (1989).
- <sup>3</sup> G. Eilenberger, Phys. Rev. **153**, 584 (1967).
- <sup>4</sup> A. Houghton, R. A. Pelcovits, and A. Sudbø, Phys. Rev. **B 40**, 6763 (1989).
- <sup>5</sup> A. A. Abrikosov, Zh. Eksp. Teor. Fiz., **32**, 1442, 1957; Sov. Phys. JETP, **5**, 1174, (1957).
- <sup>6</sup> Z. Tešanović, Phys. Rev. **B 51**, 16204 (1995).
- <sup>7</sup> A. K. Nguyen, A. Sudbø, and R. E. Hetzel, Phys. Rev. Lett. **77**, 1592 (1996).
- <sup>8</sup> X. Hu, S. Miyashita, and M. Tachiki, Phys. Rev. Lett., **79**, 3498 (1997).
- <sup>9</sup> A. K. Nguyen and A. Sudbø, Phys. Rev. **B 57**, 3123 (1998).
- <sup>10</sup> T. J. Hagenaars and E. H. Brandt, Phys. Rev. **B 56**, 11435 (1997).
- <sup>11</sup> E. Zeldov, D. Majer, M. Konczykowski, V. B. Geshkenbein, V. M. Vinokur, and H. Shtrikman, Nature **375**, 373 (1995); N. Morozov, E. Zeldov, D. Majer, and M. Konczykowski, Phys. Rev **B 54**, R3784 (1996); D. T. Fuchs, R. A. Doyle, E. Zeldov, D. Majer, W. S. Seouw, R. J. Drost, T. Tamegai, S. Ooi, M. Konczykowski, and P. H. Kes, Phys. Rev. **B 55**, R 6156 (1997).
- <sup>12</sup> M. V. Feigel'man, V. B. Geshkenbein, L. B. Ioffe, and A. I. Larkin, Phys. Rev. B **48**, 16641 (1993).
- <sup>13</sup> M. B. Salamon and J. Shi, Phys. Rev. **B 47**, 5520 (1993).
- <sup>14</sup> M. Roulin, A. Junod, A. Erb, and E. Walker, J. Low Temp. Phys., **105**, 1099 (1996); A. Junod, M. Roulin, J. Genoud, B. Revaz, A. Erb, and E. Walker, Physica C **275**, 245 (1997); M. Roulin, A. Junod, and E. Walker, Science, **273**, 1210 (1996); Physica C **282**, 1401 (1997).
- <sup>15</sup> A. Schilling, R. A. Fisher, N. E. Phillips, U. Welp, D. Dasgupta, W. K. Kwok, and G. W. Crabtree, Nature **382**, 791 (1996).
- <sup>16</sup> O. Jeandupeux, A. Schilling, H. R. Ott, and A. van Otterlo, Phys. Rev. **B 53**, 12475 (1996); A. Schilling, R. A. Fisher, N. E. Phillips, U. Welp, W. K. Kwok, and G. W. Crabtree, Phys. Rev. Lett. **78**, 4833 (1997).
- <sup>17</sup> We thank Z. Tešanović for discussions on this point.
- <sup>18</sup> R. E. Hetzel, A. Sudbø, and D. A. Huse, Phys. Rev. Lett., **69**, 518 (1992).
- <sup>19</sup> Ying-Hong Li and S. Teitel, Phys. Rev. **B 47**, 359 (1993); *ibid* **B 49**, 4136 (1994).
- <sup>20</sup> T. Chen and S. Teitel, Phys. Rev. B **55** 11766 (1997).
- <sup>21</sup> R. Cavalcanti, G. Carneiro, and A. Gartner, Europhys. Lett. **17**, 449 (1992); R. Cavalcanti, G. Carneiro, and A. Gartner, Phys. Rev. **B 47**, 5263 (1993).
- <sup>22</sup> J. Hu and A. H. MacDonald, Phys. Rev. **B 56**, 2788 (1997).
- <sup>23</sup> C. Dasgupta and B. I. Halperin, Phys. Rev. Lett. **47**, 1556 (1981).
- <sup>24</sup> L. Onsager, Nuovo Cimento Suppl., **6**, 249 (1949); P. C. Hemmer, H. Holden, and S. K. Ratkje, *The collected works of Lars Onsager*, World Scientific, Singapore, (1996) p. 1070.
- <sup>25</sup> N. Goldenfeld, *Lectures on Phase Transitions and the Renormalization Group*, Addison-Wesley Publishing Company, (1992).
- <sup>26</sup> N. Schultka and E. Manousakis, Phys. Rev. **B 52**, 7528 (1995). See also M. Friesen and P. Muzikar, cond-mat/9703135.
- <sup>27</sup> M. Franz and S. Teitel, Phys. Rev. Lett., **73**, 480 (1994); S. Hattel and J. M. Wheatley, Phys. Rev. **B 50**, 16950 (1994); Phys. Rev. **B 51**, 11951 (1995).
- <sup>28</sup> M. Kiometzis, H. Kleinert, and A. M. J. Schakel, Fortschr. Phys. **43**, 697 (1995); cond-mat/9508142.
- <sup>29</sup> S. Ryu and D. Stroud, Phys. Rev. Lett., **78**, 4629 (1997).
- <sup>30</sup> A. E. Koshelev, Phys. Rev. **B 56**, 11201 (1997).
- <sup>31</sup> B. A. Hubermann and S. Doniach, Phys. Rev. Lett., **43**, 950 (1979); D. S. Fisher, Phys. Rev. **B 22**, 1190 (1980).
- <sup>32</sup> V. J. Emery and S. A. Kivelson, Nature, **374**, 434 (1995).
- <sup>33</sup> H. Safar, P. L. Gammel, D. A. Huse, D. J. Bishop, J. P. Rice, and D. M. Ginsberg, Phys. Rev. Lett., **69**, 824 (1992).
- <sup>34</sup> H. Pastoriza, M. F. Goffman, A. Arribère, and F. de la Cruz, Phys. Rev. Lett., **72**, 2951 (1994).
- <sup>35</sup> M. J. W. Dodgson, V. B. Geshkenbein, H. Nordborg, and G. Blatter, Phys. Rev. Lett., **80**, 837 (1998); cond-mat/9712145.
- <sup>36</sup> E. H. Brandt, J. Low. Temp. Phys. **26**, 709 (1997); **26**, 262 (1997); **28**, 291 (1997).
- <sup>37</sup> M. Wallin and S. M. Girvin, Phys. Rev. **B 47**, 14642 (1993).

FIG. 1. Specific heat  $C$  per site, inplane structure factor  $S(\mathbf{k}_\perp = 2\pi/5, \pi/4)$ , helicity modulus along z-axis  $\Upsilon_z$ , and helicity modulus along x-axis  $\Upsilon_x$  as functions of temperature for the system with vortex line density  $f = 1/20$ . The inplane structure function  $S(\mathbf{k}_\perp)$  jumps discontinuously from 0.2 to 0 precisely at  $T_m = 0.531J_\perp$  indicating that the FLL melts in a first order phase transition. At the same temperature,  $\Upsilon_z$  also shows a discontinuity from 0.6 to 0, indicating that *the FLL melts directly into the incoherent vortex liquid* with no global phase coherence along the applied magnetic field direction. At temperatures above  $T_m$  there is no global phase coherence in any direction. The specific heat also shows a  $\delta$ -function anomaly precisely  $T_m$ . The broad specific heat anomaly at  $T_{Bc2} \sim 1.05J_\perp$  represents the remains of the zero-field Onsager vortex loop blowout. Note that for temperatures  $T_m < T < T_{Bc2}$  local superconducting phase coherence still exist. giving strong diamagnetic fluctuations in the liquid phase. The FLL depins from the numerical lattice at  $T_d \ll T_m$  where  $\Upsilon_x$  vanish. Thus, the FLL melting transition at  $T_m \gg T_d$  is not affected by the numerical lattice.

FIG. 2. Intensity plots of the structure function  $S(\mathbf{k}_\perp)$  for various temperatures for the system with flux-line density  $f = 1/20$ .  $k_x \in [-\pi, \pi]$  and  $k_y \in [-\pi, \pi]$  is along the horizontal and the vertical direction, respectively. The brightness in the plots is a measure of the magnitude of  $S(\mathbf{k}_\perp)$ . To enhance features we put all points where  $S(\mathbf{k}_\perp) < 0.01$  (noise level) to black and all points where  $S(\mathbf{k}_\perp) > 0.05$  to white. Precisely at  $T_m$ , the sharp Bragg-peaks in  $S(\mathbf{k}_\perp)$  are converted into Bragg-rings, characteristic of a liquid. Thus, the FLL melts into a vortex liquid within a temperature region of  $\Delta T = 0.001J_\perp$ .

FIG. 3. Internal energy per site  $E$  as a function of temperature for the system with vortex line density  $f = 1/20$ . The data are obtained from a cooling sequence using 3000000 sweeps per temperature. The internal energy has a discontinuous jump at  $T_m$  indicating a first order transition from an ordered state (FLL) to a disordered state (phase-incoherent vortex liquid). This jump in the internal energy is used to determine the latent heat (entropy jump) at the FLL melting transition. The jump in  $E$  here corresponds to a jump in the entropy per vortex line per layer  $\Delta S(f = 1/20) = 0.1k_B$ .

FIG. 4. Snapshots of the vortex configuration for the system with vortex line density  $f = 1/20$  for four temperatures,  $T/J_\perp = 0.26, 0.50, 0.54, 0.70$ . For clarification we have shown only a part of the system;  $x, y \in [0 : 20]$  and  $z \in [0 : 40]$ . For  $T = 0.26J_\perp \ll T_m$ , the flux lines form a hexagonal lattice. Although there are many thermally induced defects attached to each flux line, they are nonetheless well defined quantities. For  $T = 0.50J_\perp \lesssim T_m$ , the FLL is still intact. Although the flux lines now contain many larger defects, they are still well defined. For  $T = 0.54J_\perp \gtrsim T_m$ , the FLL has melted. For  $T \gtrsim 0.54J_\perp$ , it is seen that the flux lines are no longer well defined quantities. There exists at least one way for a flux -line to thread the system in any direction. For any vortex-configuration, therefore, there exists at least one flux line threading the sample in the direction perpendicular to the magnetic field.

FIG. 5. The inplane structure function  $S(\mathbf{k}_\perp)$  as a function of temperature for several vortex line densities  $f$ . For a given  $f$ ,  $S(\mathbf{k}_\perp)$  with the corresponding value of  $\mathbf{k}_\perp$  shows a sharp drop from  $\sim 0.2$  to 0 at a well-defined FLL melting temperature  $T_m(f)$ .

FIG. 6. The helicity modulus  $\Upsilon_z$  along the field direction as a function of temperature for several flux-line densities  $f$ . For all densities,  $\Upsilon_z$  shows a sharp drop towards zero precisely at the corresponding FLL melting temperature  $T_m(f)$ . Thus, the FLL melts directly into an incoherent vortex liquid.

FIG. 7. Monte-Carlo results for the specific heat per site of the anisotropic  $3DXY$ -model as a function of temperature for several vortex line densities  $f$ . The system sizes depends on filling fraction, as explained in the text, and  $\Gamma = 3$ . For clarity the  $n$ th curves is shifted by an amount  $0.2 * n$  upwards. For each  $f$  there is a spike at a  $f$ -dependent critical temperature  $T_m(f)$  indicating a first order phase transition.

FIG. 8. Monte-Carlo results for the specific heat of the anisotropic  $3DXY$ -model as a function of temperature for several flux-line densities. For decreasing  $f$  (decreasing magnetic field induction  $B$ ) the crossover temperature  $T_{Bc2}(f)$  increases and moves towards the zero field critical temperature  $T_{Bc2}(f = 0) = T_c$ . The broad anomaly (cusp) in the specific heat becomes sharper and the maximum height of the cusp increases. Thus, for decreasing  $f$  the specific heat evolves smoothly to the zero field specific heat singularity at  $T_c$ . The spike in the specific heat at  $T_m(f) \ll T_{Bc2}(f)$  each graph is hidden in the noise of the other graphs and is therefore hard to recognize in this particular figure. While in zero magnetic field the vortex loop blowout is the mechanism for the second order phase transition at  $T_c$ , in finite magnetic field the vortex loop blowout at  $T_{Bc2}(f)$  is only a crossover. The phase transition in systems with finite vortex line densities take place at a lower temperature,  $T_m(f)$ , where the vortex line lattice melts.

FIG. 9. Monte-Carlo results for the specific heat of the anisotropic  $3DXY$ -model in zero magnetic field, for various system sizes  $L \times L \times L$  with  $L = 32, 48, 64, 72, 96$ , and two values of the anisotropy,  $\Gamma = 1$  and  $\Gamma = 3$ , scaled according to Eq. 6. Here,  $t = (T - T_c)/T_c$ . The region of data collapse gives the width of the critical region. Note that this region is slightly for  $\Gamma = 3$  than for  $\Gamma = 1$ .

FIG. 10. Monte-Carlo results for the specific heat of the anisotropic  $3DXY$ -model for a number of filling fractions  $f$  given by  $1/f = 12, \dots, 128$  with corresponding system sizes as explained in text, and anisotropy  $\Gamma = 3$ , scaled according to Eq. 7. The results are in good agreement with the experimental results of Schilling *et al.*, and Junod *et al.*

FIG. 11. The entropy jump per vortex line per layer  $\Delta S(f)$  at the FLL melting transition for several vortex line densities  $f$ . The filled circles represent the results obtained with a  $T$ -independent Hamiltonian, Eq. 1. The open circles represent the results obtained including a  $T$ -dependent prefactor in the Hamiltonian. We see that  $\Delta S(f)$  essentially does not depend on  $f$  in this regime of filling fractions  $f$ , regardless of whether  $T$ -dependent prefactors are included in the Hamiltonian or not. The inset shows the enhancement factor in Eq. 14.

FIG. 12. The helicity modulus perpendicular to the field direction  $\Upsilon_x$  as a function of temperature for several vortex line densities  $f$ . For each  $f$ ,  $\Upsilon_x$  vanishes at a temperature  $T_d(f)$  significantly lower than the corresponding FLL melting temperature  $T_m(f)$ . The artificial pinning potential of the numerical lattice therefore does not affect the FLL melting transition at  $T_m(f) \gg T_d(f)$ .

FIG. 13. The f-T phase diagram for the uniformly frustrated 3d XY model. The applied field is along the crystal c-axis, the anisotropy parameter  $\Gamma = 3$ . The FLL exhibits global phase coherence along the applied field direction. The FLL phase is separated from the incoherent flux-line liquid phase by the melting line  $T_m(f)$ . The melting transition is a first order phase transition with an entropy jump  $\Delta S(f) \sim 0.1k_B$  for the anisotropy  $\Gamma = 3$  and field regime considered in this paper. In the incoherent vortex liquid phase  $T_m(f) < T < T_{Bc2}(f)$ , there is only local, but no global, phase coherence in any direction. At finite fields, between the incoherent vortex liquid and the normal metal phase, there exists a broad crossover region where a blowout of thermally induced closed vortex loops takes place, eventually also destroying superconductivity on short length scales. The width of the crossover regime is obtained from scaling behavior of the specific heat. Another, consistent, method of obtaining this width, is to estimate the temperature regime which corresponds to an uncertainty of 10% in the maximum value of the specific heat anomaly at  $T_{Bc2}(f)$ . Since this anomaly becomes broader with increasing field, the cross-over region becomes wider. This is also confirmed from the scaling results for the specific heat.

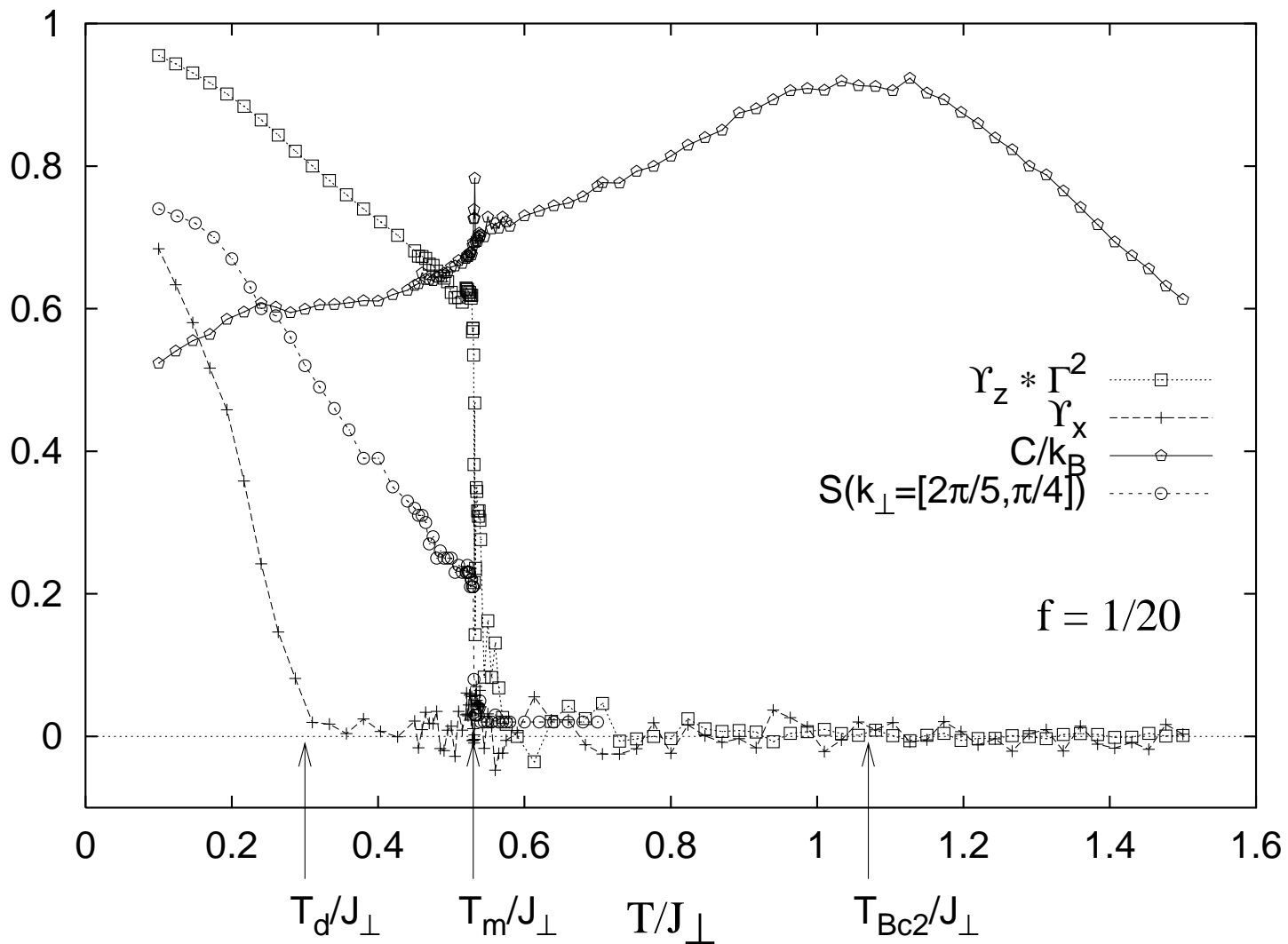
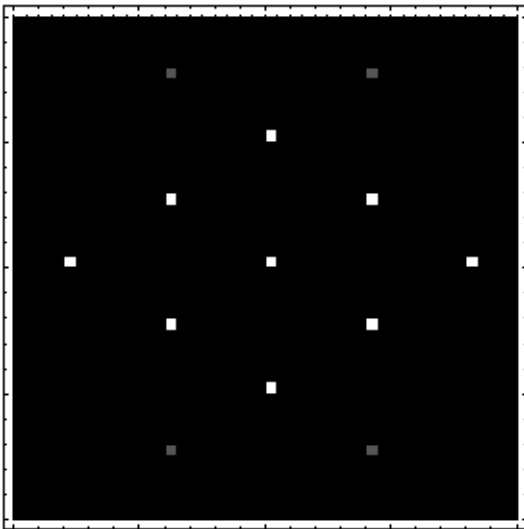
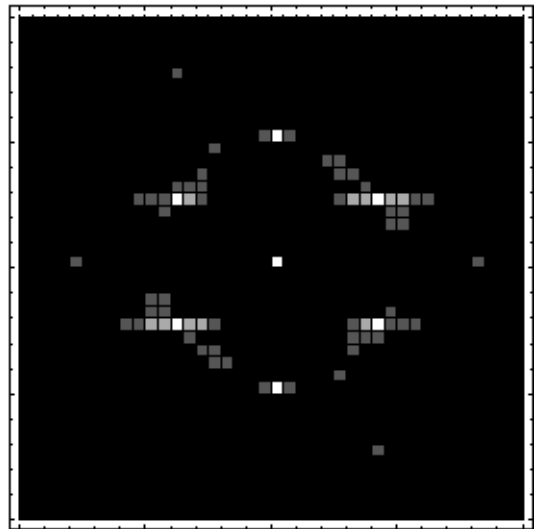


Figure 1

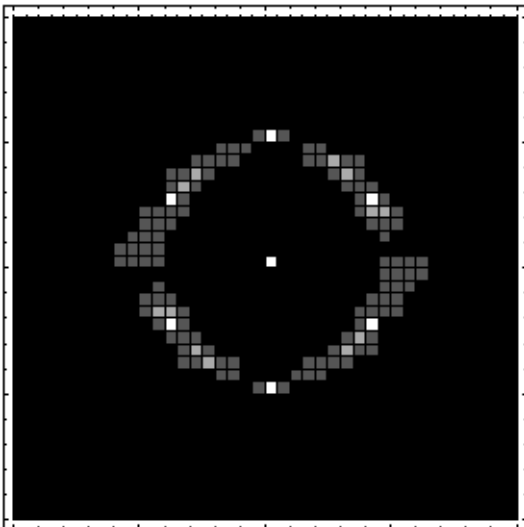


$$T = 0.450J_{\perp} < T_m$$

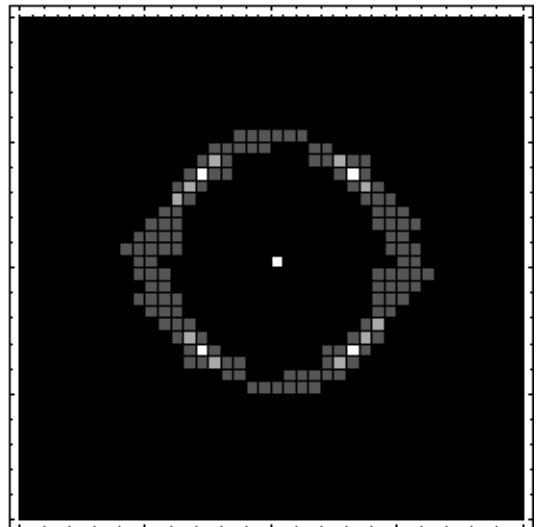


$$T = 0.530J_{\perp} \lesssim T_m$$

$$f = 1/20$$



$$T = 0.531J_{\perp} = T_m$$



$$T = 0.532J_{\perp} \gtrsim T_m$$

Figure 2



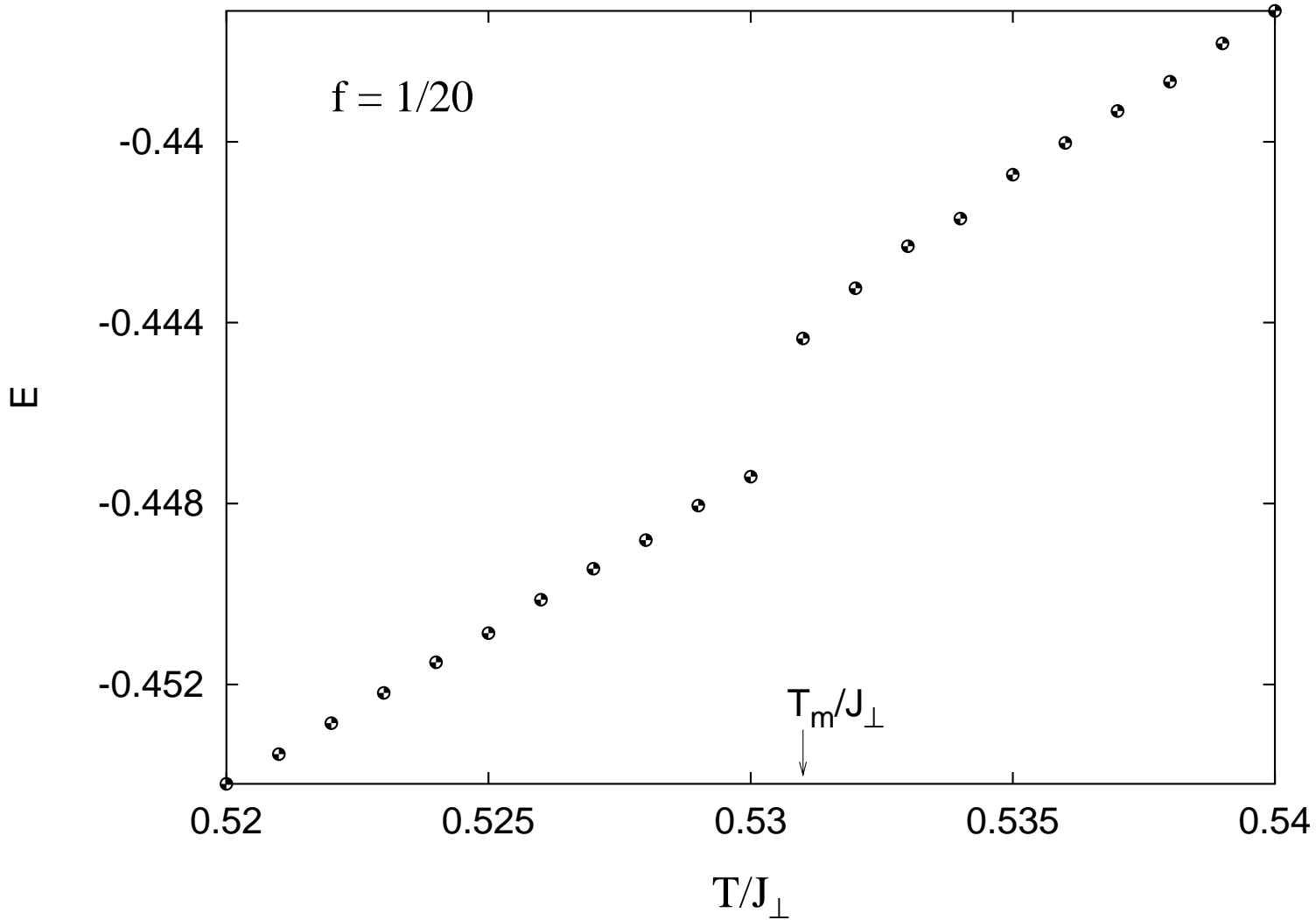


**Figure 3**

$$\begin{aligned}
 f &= 1/20 \\
 T_m &= 0.53J_{\perp} \\
 T_{Bc2} &= 1.05J_{\perp}
 \end{aligned}$$

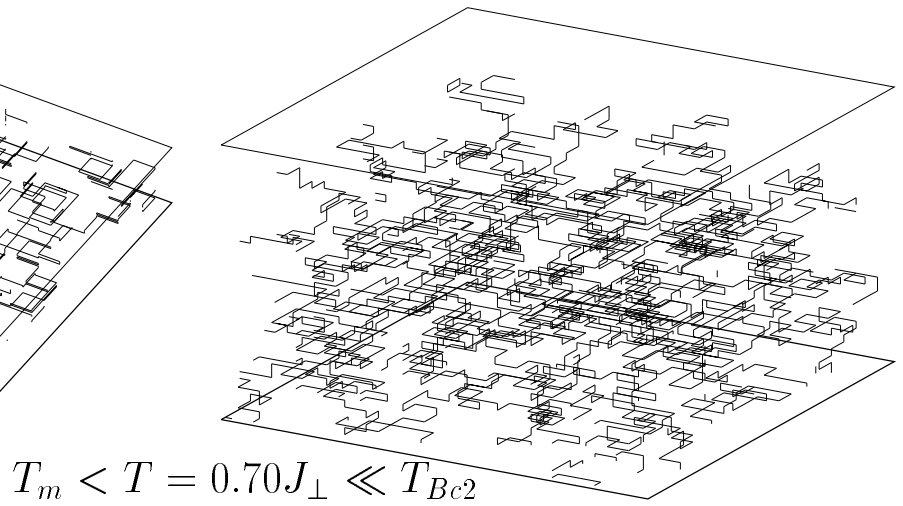
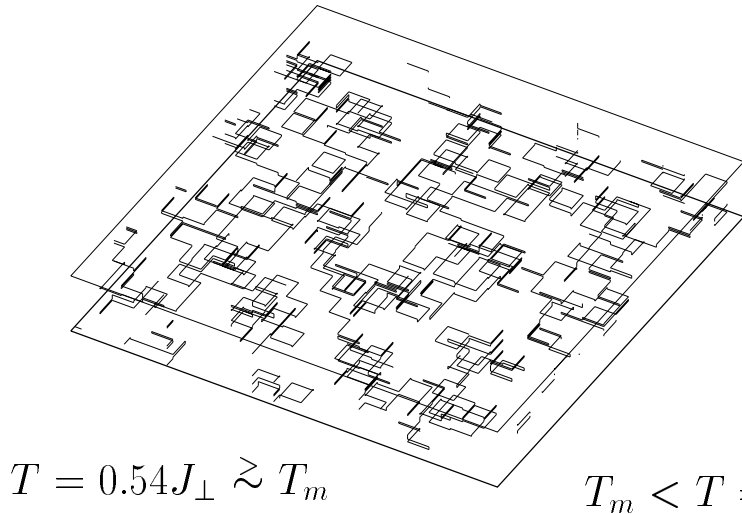
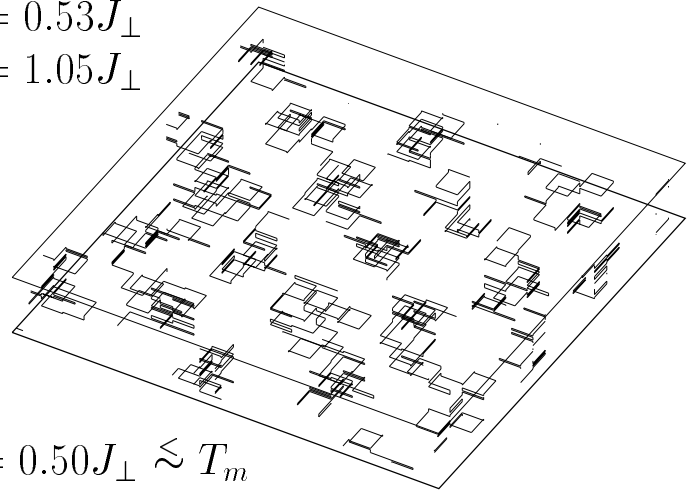
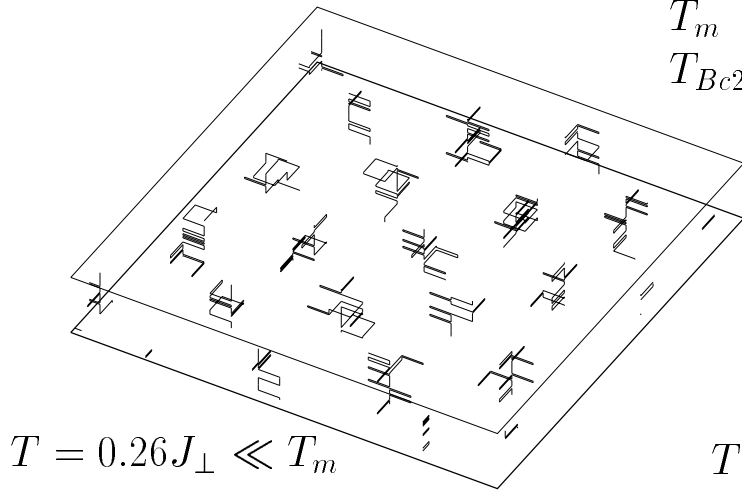


**Figure 4**

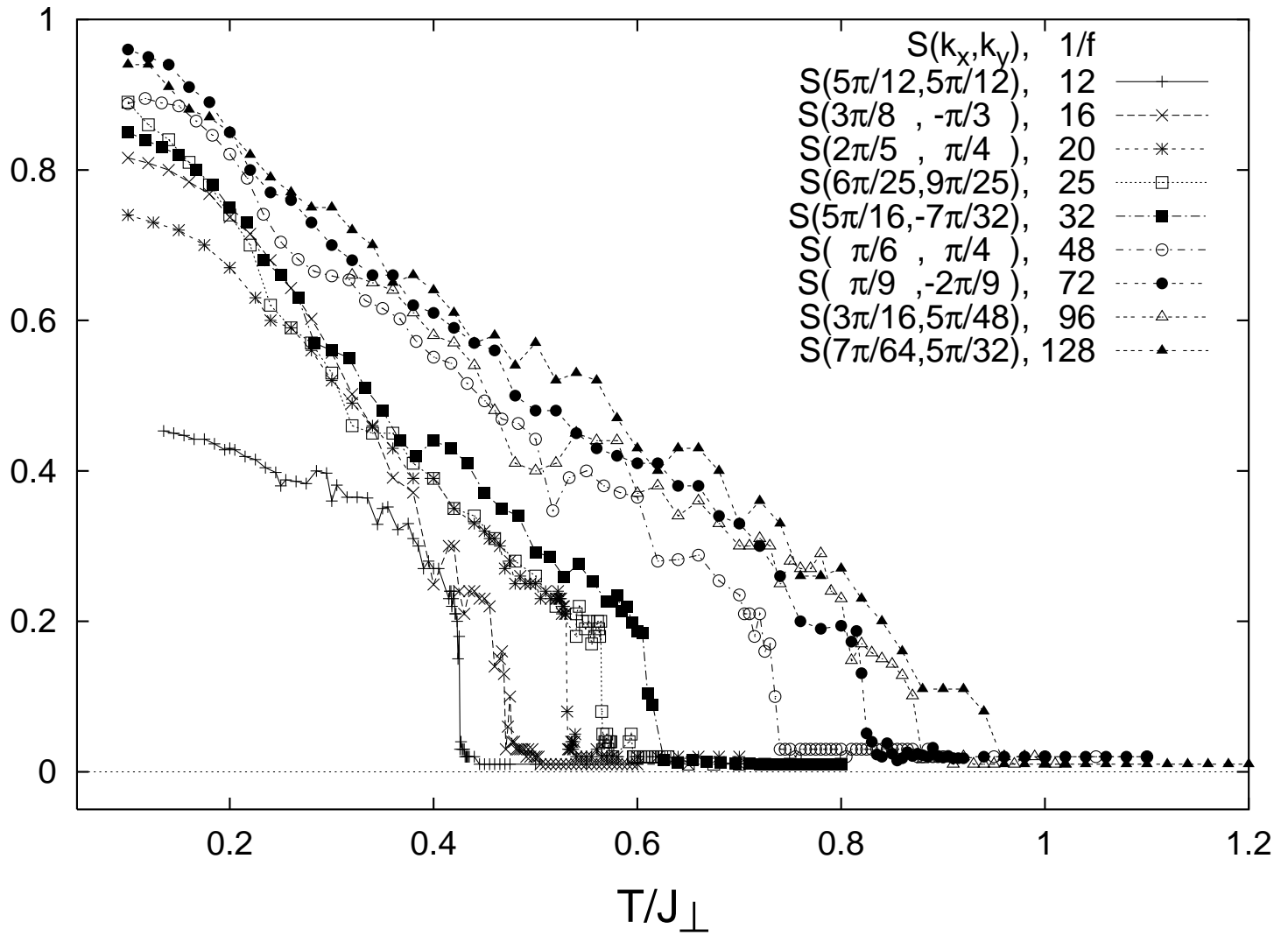
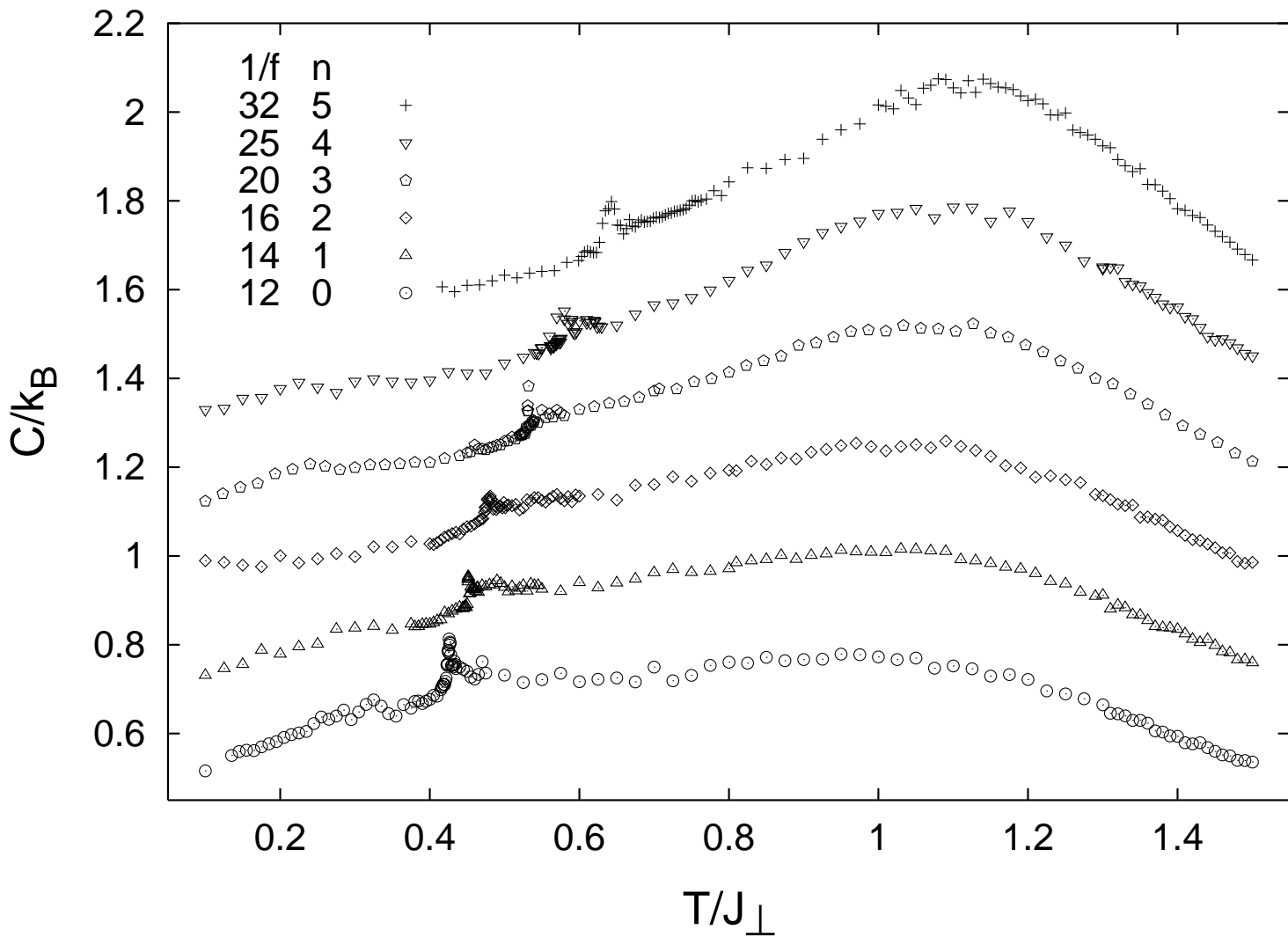


Figure 5



**Figure 6**

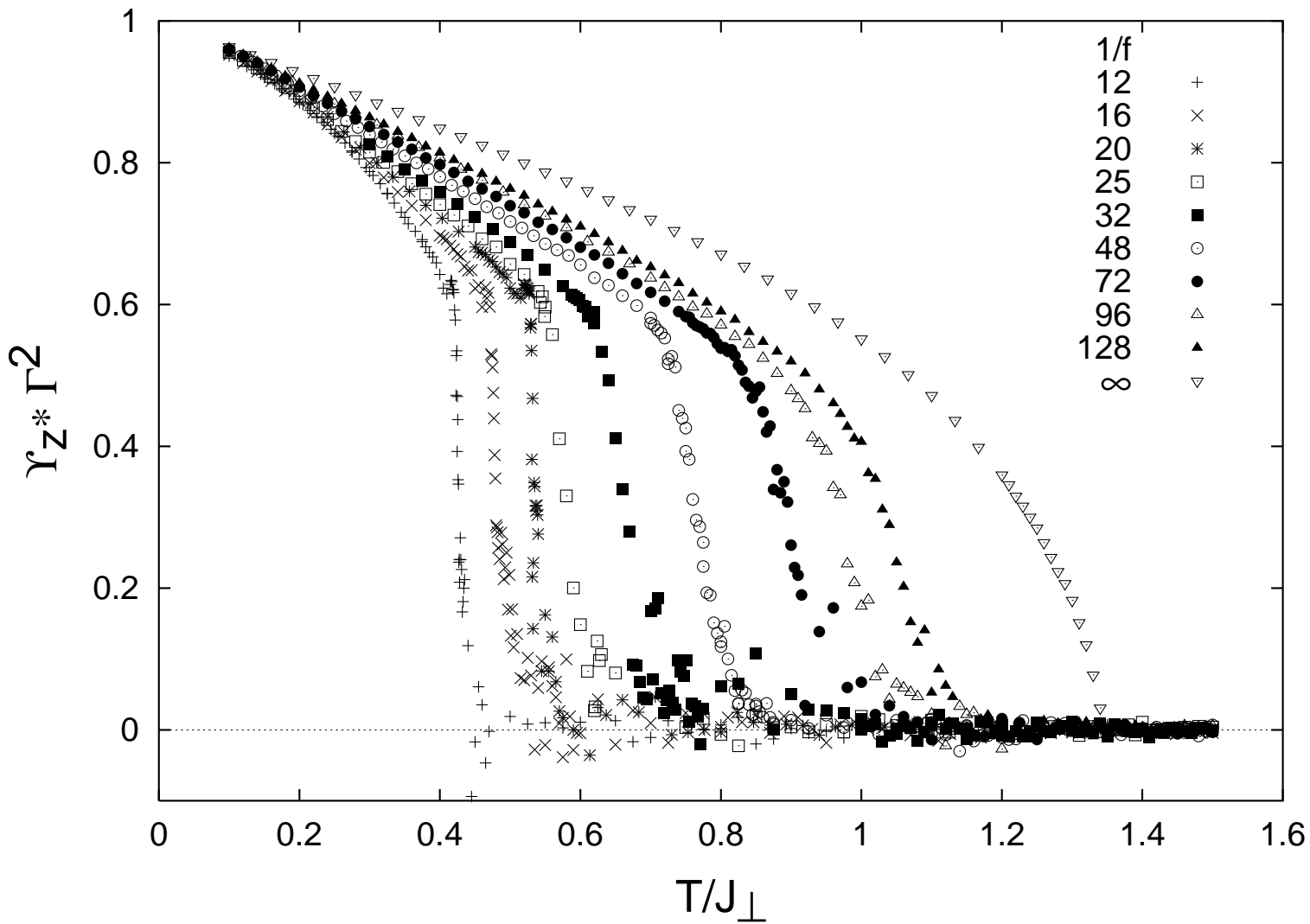


Figure 7

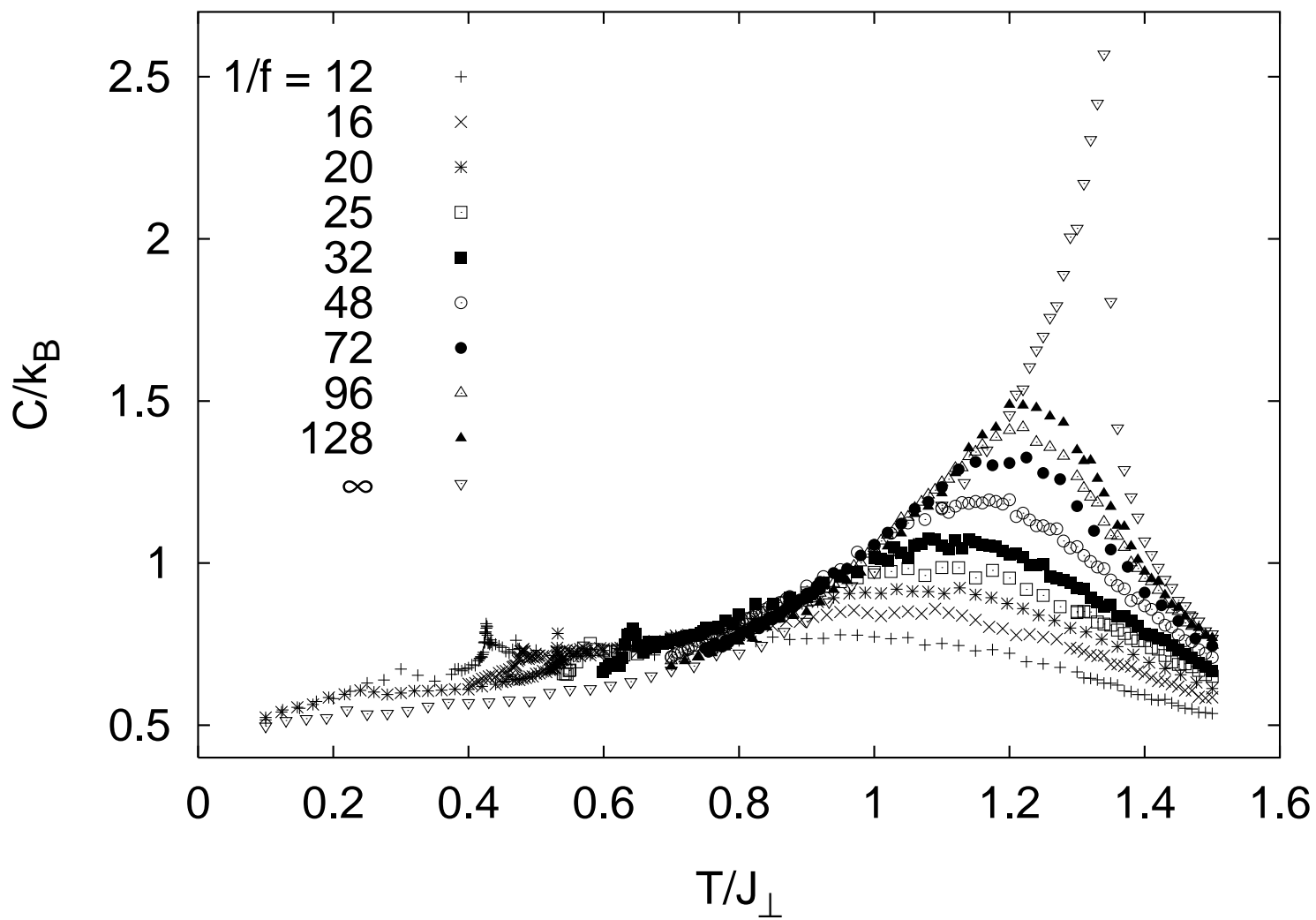


Figure 8

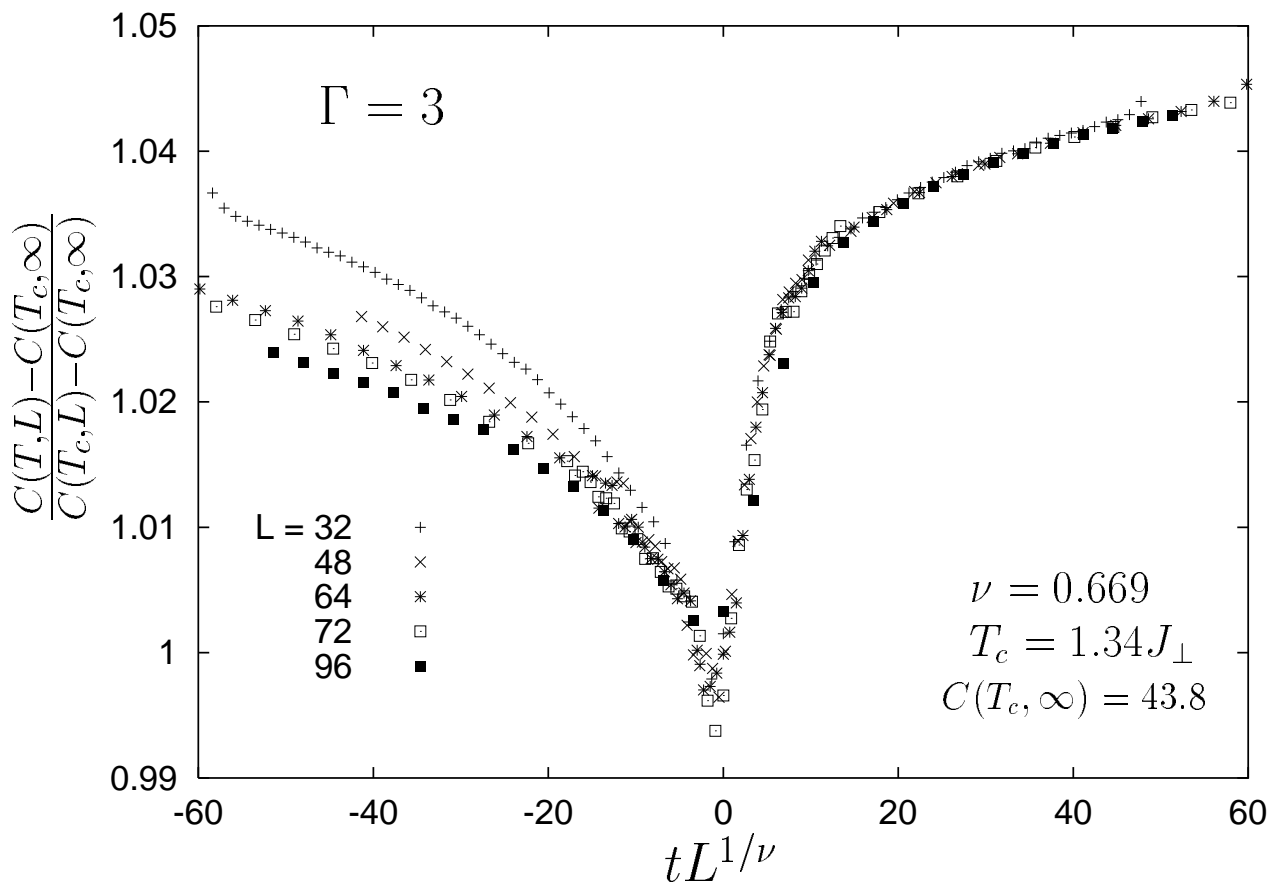
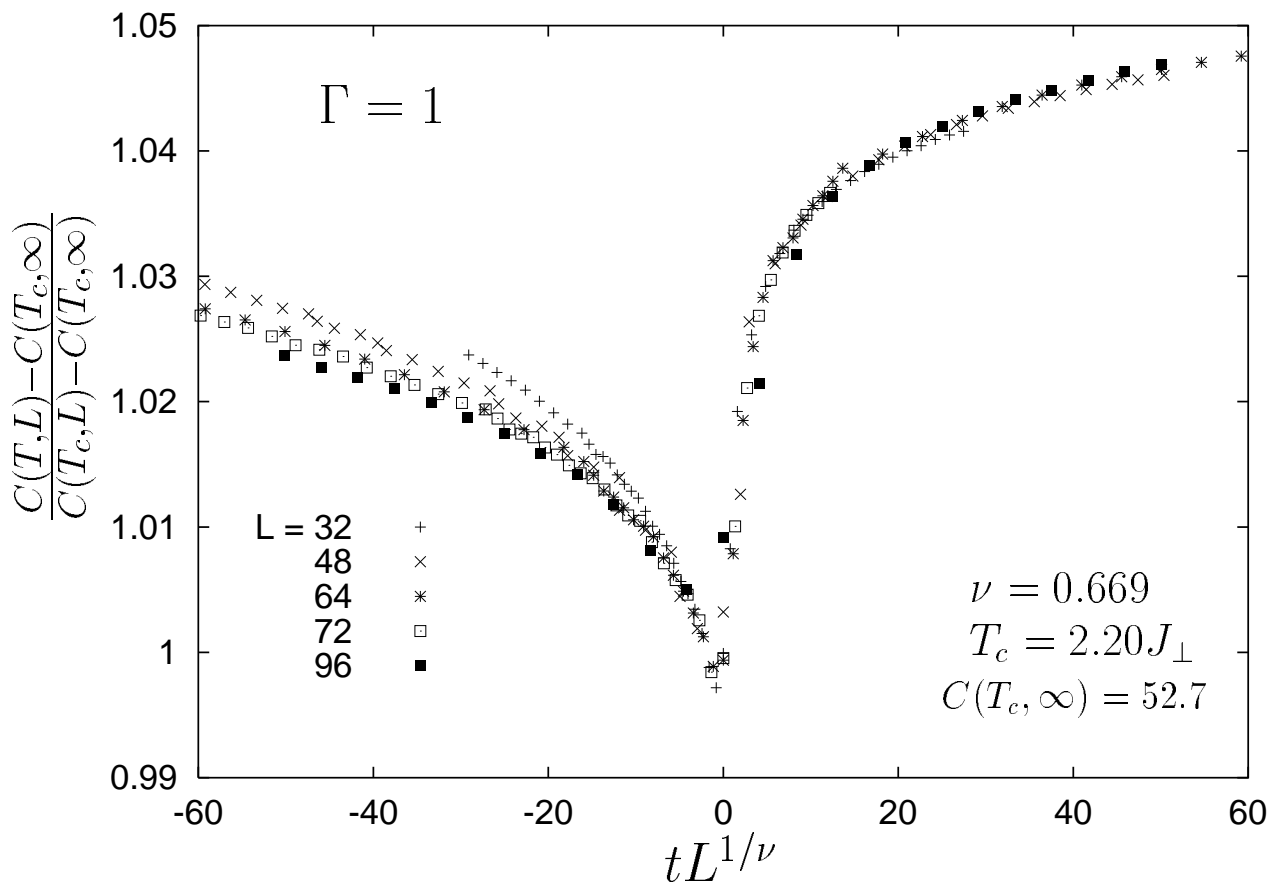


Figure 9

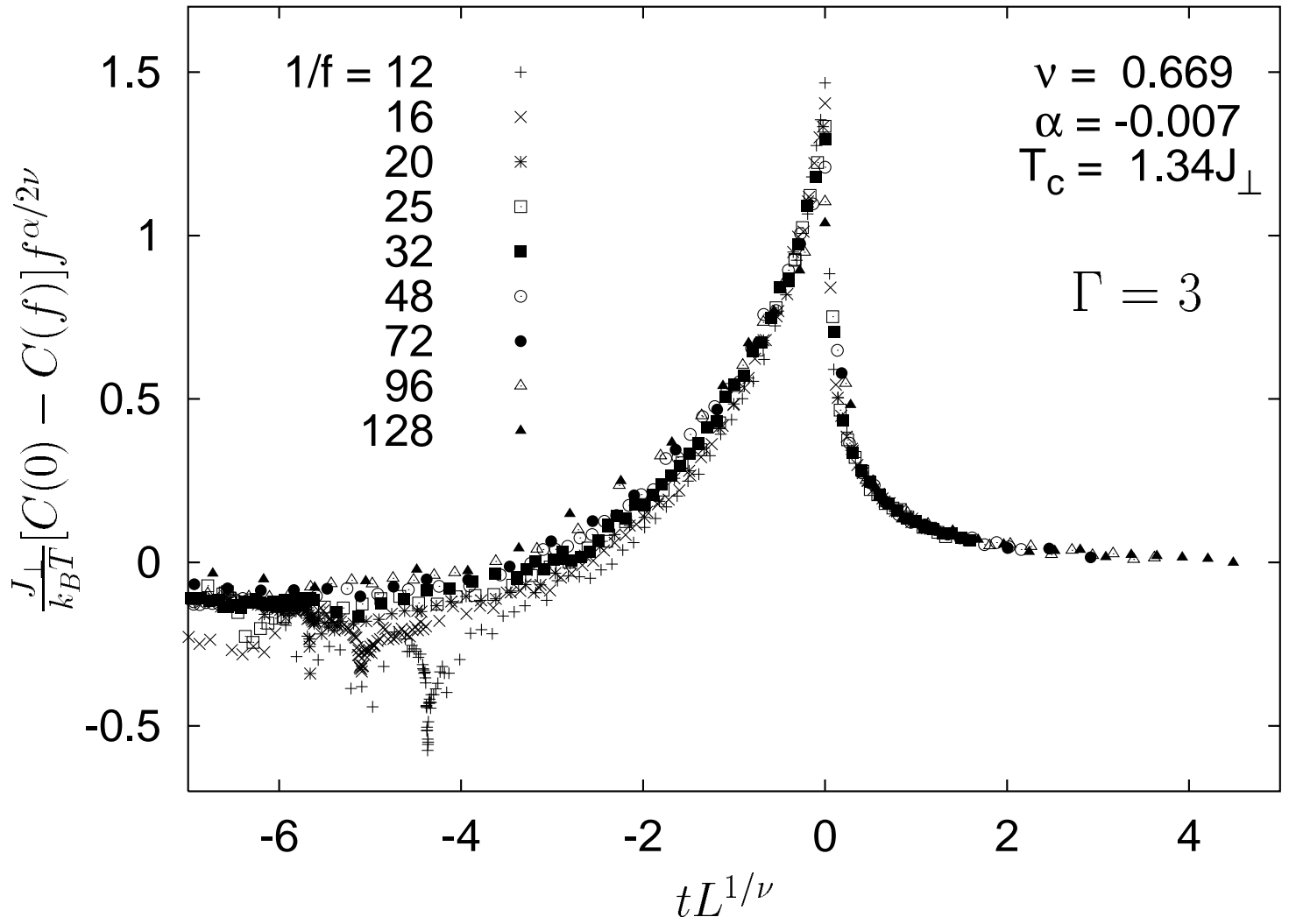


Figure 10



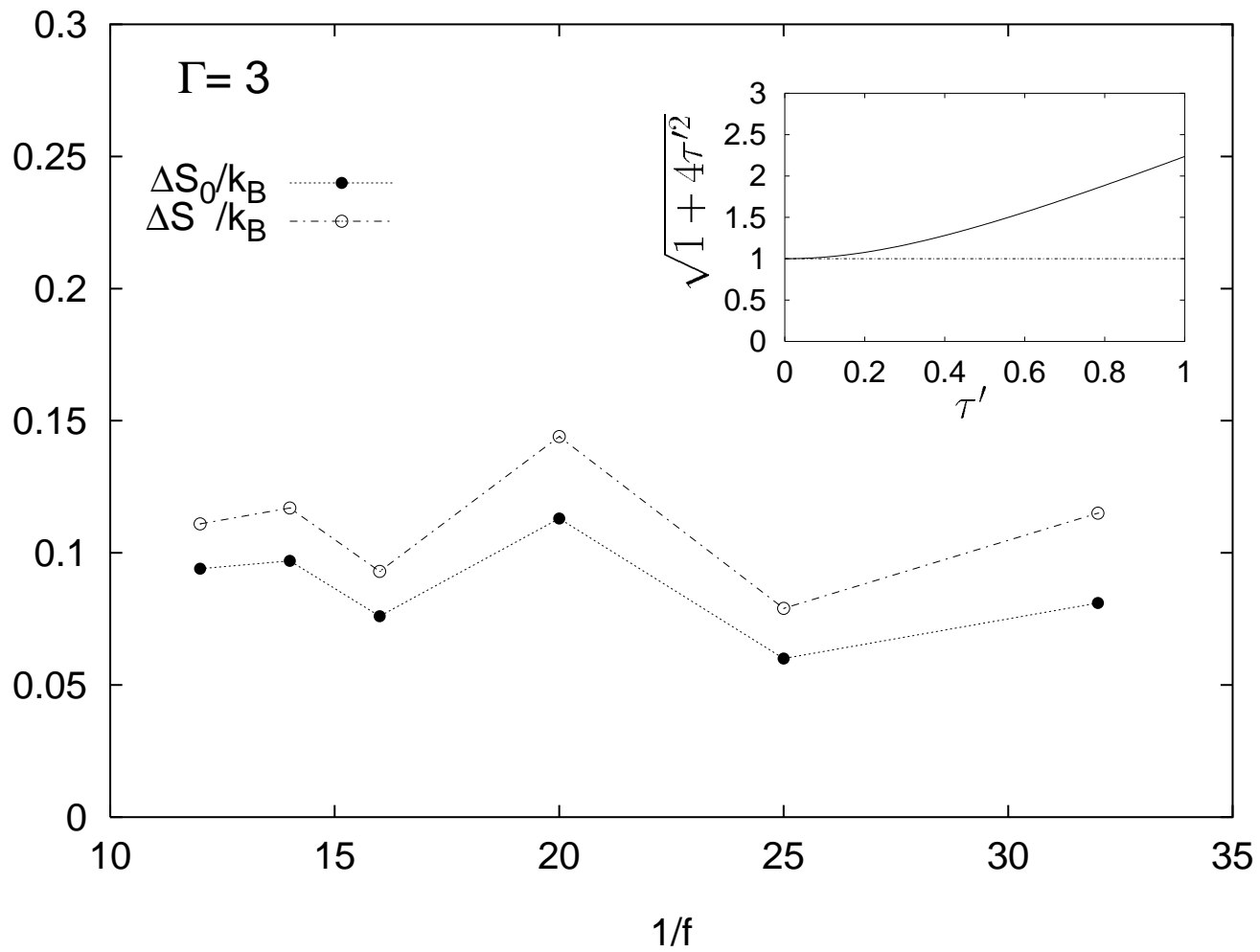


Figure 11

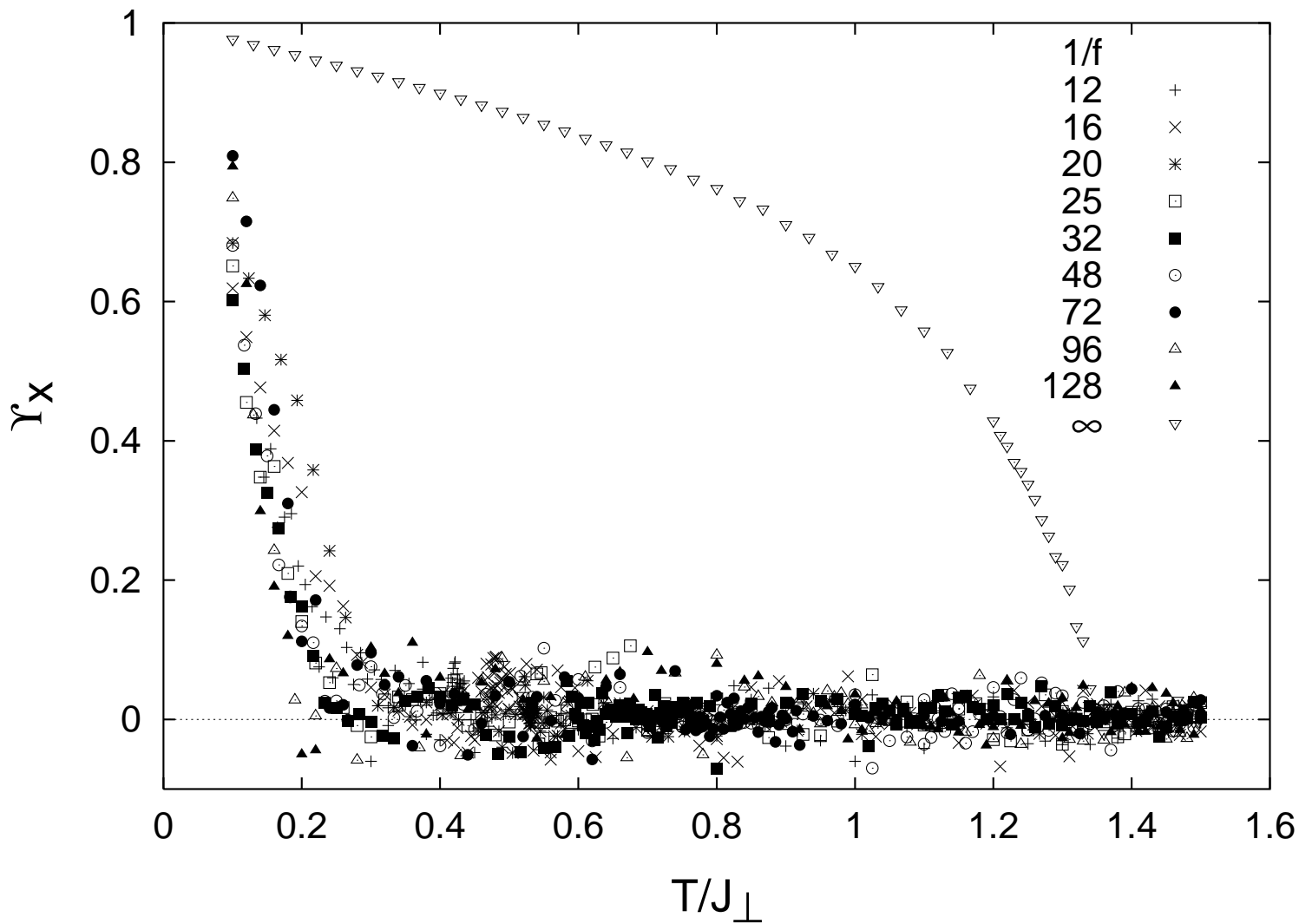
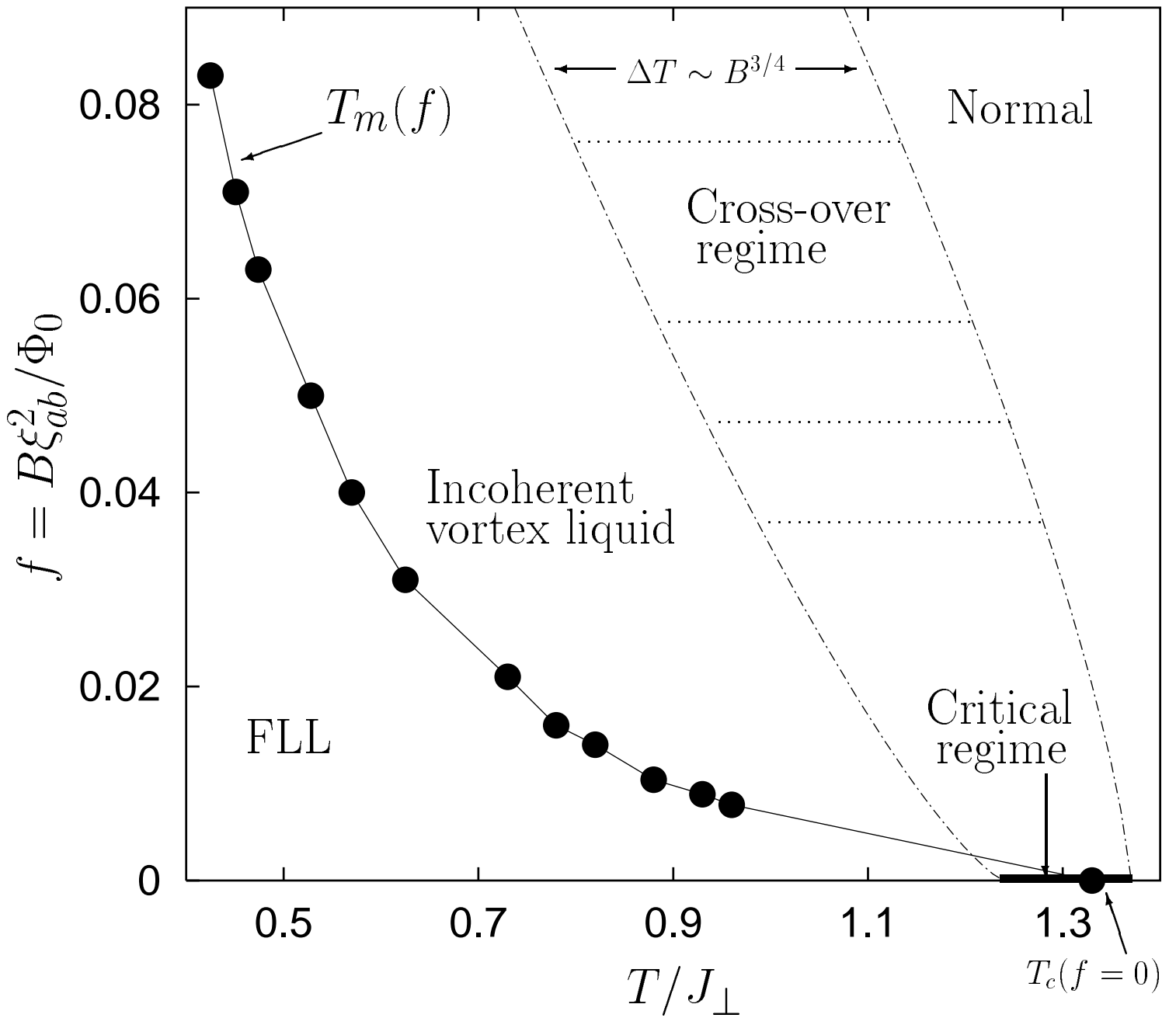


Figure 12



**Figure 13**